RESEARCH ARTICLE

Scales of columnar jointing in igneous rocks: field measurements and controlling factors

György Hetényi · Benoît Taisne · Fanny Garel ·
Étienne Médard · Sonja Bosshard · Hannes B. Mattsson

Abstract Columnar jointing is a common feature of solidified lavas, sills and dikes, but the factors controlling the characteristic stoutness of columns remain debated, and quantitative field observations are few in number. In this paper, we provide quantitative measurements on sizing of columnar joint sets and our assessment of the principal factors controlling it. We focus on (1) chemistry, as it is the major determinant of the physical (mechanical and thermal) properties of the lava, and (2) geology, as it influences the style of emplacement and lava geometry, setting boundary conditions for the cooling process and the rate of heat loss. In our analysis, we cover lavas with a broad range of chemical compositions (from basanite to phonolite, for six of which we provide new geochemical analyses) and of geological settings. Our field measurements cover 50 columnar jointing sites in three countries. We provide reliable, manually digitized data on the size of individual columns and focus the mathematical analysis on their geometry (23,889 data on side length, of which 17,312 are from full column sections and 3,033 data on cross-sectional area and order of polygonality). The geometrical observations show that the variation in characteristic size of columns between different sites exceeds one order of magnitude (side length ranging from 8 to 338 cm) and that the column-bounding polygons' average order is less than 6. The network of fractures is found to be longer than required by a minimum-energy hexagonal configuration, indicating a non-equilibrium, geologically quick process. In terms of the development and characteristic sizing of columnar joint sets, our observations suggest that columns are the result of an interplay between the geological setting of emplacement and magma chemistry. When the geological setting constrains the geometry of the emplaced body, it exerts a stronger control on characteristic column stoutness. At unconstrained geometries (e.g. unconfined lava flows), chemistry plays the major role, resulting in stouter columns in felsic lavas and slenderer columns in mafic lavas.

G. Hetényi (✉) · S. Bosshard · H. B. Mattsson
Department of Earth Sciences, ETH Zürich,
Clausiusstrasse 25,
8092 Zurich, Switzerland
e-mail: gyorgy.hetenyi@erdw.ethz.ch

B. Taisne · F. Garel
Institut de Physique du Globe de Paris, Sorbonne Paris Cité,
Université Paris Diderot, CNRS UMR 7154,
1 rue Jussieu,
75238 Paris cedex 5, France

É. Médard
Laboratoire Magma et Volcans, Clermont Université,
Université Blaise Pascal,
BP 10448, 63000 Clermont-Ferrand, France

É. Médard
CNRS, UMR 6524, LMV,
63038 Clermont-Ferrand, France

É. Médard
IRD, R 163, LMV,
63038 Clermont-Ferrand, France

Introduction

Columnar jointing is a feature that occurs worldwide in a variety of rocks (e.g. Spry 1962). It is most often associated with igneous bodies that are divided into columns along a network of polygonal fractures. Columnar joints have also been reported in sedimentary rocks (loess, baked clays, sandstones, e.g. Spry and Solomon 1964) and pyroclastic deposits (ignimbrites, e.g. Gilbert 1938). Columnar jointing is always associated with a decrease in volume, creating tensional stresses within the body. This volume decrease can be due to evaporation (natural desiccation of clay sediments, e.g. Konrad and Ayad 1997; cracking in cornstarch experiments, e.g. Goehring and Morris 2005) or to thermal contraction (cooling lava body, e.g. Mallett 1875).

Columnar joint formation

Columnar jointing has long been described and discussed in indigenous oral traditions. One of these legends, from the Kiowa Indians, related to the Devils Tower in Wyoming (USA) tells the story of seven girls who played in a field, away from their village. Suddenly, a couple of bears attacked them, and the girls could not escape in any direction. They jumped on a big, flat rock and started to pray to the Spirit of the rock to save them. The rock suddenly started to grow and reached the sky: The girls became stars (the Pleiades, a.k.a. the Seven Sisters), and the traces of the bears' claws are preserved as the vertical striae (the joints between the columns) on the sides of Devils Tower (Hédervári 1981; http://www.scienceviews.com/parks/devil stowerlegends.html, accessed on 12 August 2011).

Scientific publications on columnar jointing date back to Bulkeley's (1693) paper, rapidly followed by several others at the end of the seventeenth century (Tomkeieff 1940 references these old works). The origin of columnar jointing was an important issue that opposed neptunists and plutonists. Neptunists, such as A. G. Werner, argued that all rocks, including the columnar jointed basalt at the castle of Stolpen, Germany, were deposited from water (Schmincke 2004). The volcanic origin of basalt was later demonstrated by Nicolas Desmarest at the end of the eighteenth century, after a careful observation of columnar jointed lava flows in the Massif Central, France (Demarest 1774, 1777).

Proposed physical mechanisms for columnar joint formation include crystallisation around nucleation centres (concretion), convection cells, contractional cooling (see, e.g. Tomkeieff 1940 and Spry 1962 for reviews) and large-scale constitutional supercooling (Guy and Le Coze 1990; Gilman 2009; Guy 2010). The currently most widely accepted view for columnar jointing is contractional cooling, first proposed by Raspe (1776), which states that the network of fractures forming the column boundaries develops due to mechanical stress buildup while the lava cools and contracts. This idea stands at the origin of numerous papers with different investigation methods, including in situ observation of columnar jointing formation (Peck and Minakami 1968), numerical models using thermal and/or mechanical equations (Jaeger 1961; Long and Wood 1986; DeGraff et al. 1989; Budkewitsch and Robin 1994; Lore et al. 2000, 2001; Kattenhorn and Schaefer 2008) and analogue experiments with starch desiccation (Müller 1998; Toramaru and Matsumoto 2004; Goehring and Morris 2005; Goehring et al. 2006, 2009).

We describe below how the fracture network develops according to the contractional cooling model. Heat loss occurs through the boundaries of the lava body, i.e. bedrock and air in the case of a simple lava flow. The lava cools conductively and tends to decrease its volume, building up stresses that can be partially released by viscoelastic relaxation. This is possible while the temperature is higher than the glass transition temperature T_G. Below this temperature, effective stress begins to accumulate, and when it overcomes the tensile strength of the rock, fractures will initiate perpendicularly to the isotensile-stress surface, which is often identical to an isothermal surface, i.e. parallel to the cooling surface (Spry 1962). The propagation of a single fracture towards the interior of the lava body proceeds until it reaches the T_G isotherm (Budkewitsch and Robin 1994), above which it is possible to create cracks only when considering high energy release (Büttner et al. 2006). Then the system remains stable until T_G migrates downwards by cooling (Ryan and Sammis 1981), potentially by the enhanced convective heat evacuation through the fracture network (Budkewitsch and Robin 1994). These downwards propagating steps create the so-called chisel marks that are parallel bands of crack advance observed on the sides of columns, sometimes with a plumose pattern (e.g. Woodworth 1896).

Spacing of columnar joints

Most studies agree that the length of a polygon-bounding fracture segment is a function of the cooling rate $\partial T/\partial t$ (Tomkeieff 1940; DeGraff et al. 1989; Budkewitsch and Robin 1994; Lore et al. 2001). Slower cooling creates wider (stouter) columns; faster cooling creates narrower (slenderer) columns. Moreover, since the width of the chisel marks depends on the spatial (vertical for lava or sill) gradient of temperature $\partial T/\partial x$, the column width and striae width are inter-related (Ryan and Sammis 1978; Grossenbacher and McDuffie 1995). Finally, since for a given magma composition glass content is usually proportional to the cooling rate (slower cooling results in higher crystallinity; faster cooling results in increased glass content of the rock), lavas

solidifying into glassier rocks are expected to have slenderer columns than more crystalline lavas.

This current understanding of columnar joint formation by contractional cooling qualitatively links cooling rate and mean joint length through the balance of stresses. The possible range of columnar joint length L observed in nature spans at least one order of magnitude as demonstrated by three basalts analysed by Ryan and Sammis (1981): $L=25$ cm at the Boiling Pots (Hawaii), $L=80$–100 cm at the first Watchung Basalt (New Jersey) and $L=170$–230 cm at the prehistoric Makaopuhi lava lake (Hawaii). The question of columnar joint scaling therefore requires: (1) an assessment of the physical properties controlling the cooling rate and the behaviour of the lava body and (2) quantitative analysis of column geometry, measurements in the field and their interpretation in terms of chemistry and geological setting.

Motivation

We propose to analyse two likely factors in controlling the cooling rate and hence columnar joint sizing (Fig. 1): (1) the geometry of the magma or lava body, as it defines the amount and shape of surfaces where heat can be exchanged with the environment, and (2) chemical composition, as it is the primary parameter controlling physical properties (viscosity, crystallinity etc.) of the emplaced body. These two controlling factors may not be fully independent, as the physical properties of the magma (controlled by its chemistry) may also affect its emplacement type. However, we have tried to separate the effects by comparing similar emplacement types with lavas and intrusions of different composition and vice versa.

Earlier work on the effects of igneous body geometry and chemistry

The geometry of the cooling magma or lava body is the combined result of its geological setting and the environment, and it defines the boundary conditions of the cooling process (Fig. 1). It has been studied by Jaeger (1961), who concluded that geometry is very influential in shaping the isotherms and therefore the columns. Later papers focus on relationships between isotherms and joints and rarely mention body geometry (e.g. Hull and Caddock 1999, in relation with silica sol-gels; Kattenhorn and Schaefer 2008, in numerical modelling of inflated lava flows). We refocus on cooling geometry by classifying our field observations according to the geometry of the emplaced magma or lava as reconstructed in the literature in order to regroup sites where the cooling conditions were comparable (e.g. lava flows, intrusive bodies etc.). The groups are described in detail in "Geometry of cooling magma bodies" Section, followed by description of the visited columnar jointed rock sites in "Field data of columnar jointing sites: geological setting and chemistry" Section.

The chemical composition affects the thermal and mechanical properties of the rock (Fig. 1) and is therefore a potential key parameter controlling the cooling rate and the fracturing of the lava body. It is, however, poorly mentioned, if not disregarded in the literature. Spry's (1962) classical paper only mentions (p. 197) that "no relation is known to exist between compositional and textural changes in a flow and the morphology of the columns". An earlier publication (Sosman 1916) states that "it should be noted, however, that the composition of the rock may have a considerable effect on the size of columns under given

Fig. 1 Scheme of the research plan for revealing the characteristic spacing of columnar joints. See text, especially Proposed approach to link lava geometry and chemistry to joint spacing Section for description
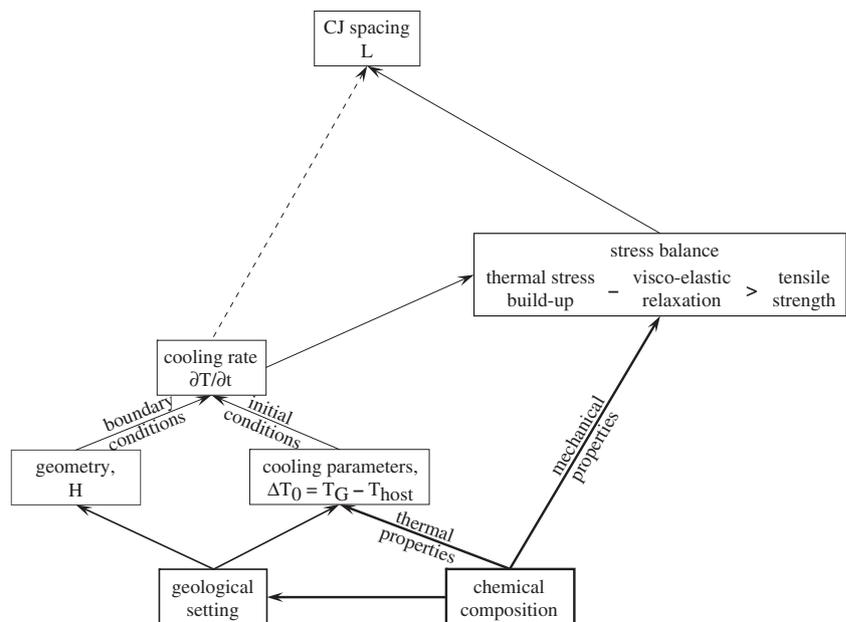
conditions of cooling, the more salic rocks forming larger columns than the more femic rocks". Since the overwhelming majority of studies on columnar joints focus on basaltic rocks, our goals included analysis of columnar jointed igneous rocks with as many different chemical compositions as possible and investigation of systematic variations in their size.

Proposed approach to link lava geometry and chemistry to joint spacing

The rationale of our study is summarized (Fig. 1) and relates geometry of the emplaced body and chemical composition of the magma to the whole-body cooling rate and ultimately to characteristic column sizes. We hereafter describe the potential ways in which these two factors may control the development of columnar jointing.

The local cooling rate, commonly inferred to be the sole control on the size of columns (Tomkeieff 1940; DeGraff et al. 1989; Budkewitsch and Robin 1994; Lore et al. 2001; dashed arrow in Fig. 1), acts through the balance of stresses. We note that in this balance, one needs to take into account:

– The thermal stress that accumulates due to the shrinkage resulting from cooling (e.g. Spry 1962):

$$\sigma_{ther} = E \cdot \alpha \cdot \Delta T / (1 - \nu), \qquad (1)$$

where E is Young's modulus, ν is the Poisson's ratio, α is the thermal expansion coefficient and ΔT is the temperature difference between the external temperature (air, water, host rock) and the glass transition temperature T_G (i.e. the temperature below which the rock is able to build up stresses, e.g. Zarzycki 1982)
– The viscoelastic relaxation of stress with time (e.g. Turcotte and Schubert 2002):

$$\sigma = \sigma_0 \cdot e^{-E \cdot t / (2 \cdot \eta)}, \qquad (2)$$

where t is time and η is viscosity
– The tensile strength of the rock σ_{tens}

The rock fractures when the total accumulated stress (thermal stress partially relieved by viscoelastic creep) exceeds the tensile strength (Fig. 1). Therefore, the slower the local cooling, the lower the temperature at which sufficient stresses accumulate; consequently, the lower the frequency of fractures (both in time and in space) and hence theoretically the larger the columns.

Both the cooling rate and the different stresses are potentially influenced by the geometry and the chemical composition of the emplaced magma (Fig. 1). The geometry of the magma body determines the *boundary conditions* (Fig. 1) for cooling and hence the whole-body cooling rate. The geometry of the magma body itself varies, depending on whether it is emplaced as intrusive bodies (e.g. dykes, sills,

laccoliths etc.), or extrusive bodies (e.g. lava flows, lava domes, lava lakes) (see Geometry of cooling magma bodies Section). The *initial condition* (Fig. 1) of cooling is dependent on emplacement setting (cooling through air for a lava lake or flow's top, cooling through host rock for an intrusive body). Complications result from successive phases of magma input into a still hot environment (Jaeger 1961) and from the chemical composition of the magma which determines its thermal properties (Fig. 1), especially its glass transition temperature T_G below which it becomes able to accumulate stress. The chemical composition of the magma also has a strong influence on its viscosity η and tensile strength σ_{tens} and therefore on the balance of stresses of the solidifying magma (Fig. 1).

We suspect that the influences of magma geometry and chemical composition are not independent, as the latter may affect the former. For example, a more viscous felsic lava flow spreads less and tends to be thicker than a relatively more fluid basaltic one of the same volume, spreading over a larger area (e.g. Walker 1967, 1973; Huppert et al. 1982).

The next sections (1) assess the importance of magma body geometry and chemical composition on the development of columnar jointing in a qualitative way (Assessment of the main controlling factors Section), (2) describe field observations (Field data of columnar jointing sites: geological setting and chemistry Section) and geometry measurements (Characterisation of the joint-bounded columns Section) and (3) interpret the findings in a physical and geological framework (Assessing the influence of body geometry and chemistry on columnar jointing size Section).

Assessment of the main controlling factors

Compositional control: variations in the physical properties of magma

Assessment of physical properties through which chemical composition exerts control on cooling and stresses of magma is done qualitatively in terms of variations as a function of the chemical composition of the lava. For simplicity, we do not consider cases with potential chemical variations with time.

The largest change in physical properties is in viscosity (orders of magnitude, e.g. 10^5 Pa s for a rhyolite, $10^{2.5}$ Pa s for an andesite and $10^{1.5}$ to $10^{0.75}$ for two basalts at 1,300°C in Murase and McBirney 1973), with felsic rocks being much more viscous than mafic ones. Equation 2 suggests slower decay of stresses and hence smaller columns in more felsic rocks, but the opposite is observed in the field (Varet 1971). This can be explained with (1) the lower ΔT (Eq. 1; Fig. 1) (solidifying felsic lavas are typically emplaced much colder than mafic ones) and hence lower total stress in more felsic rocks and (2) slower

cooling due to thicker flows that more viscous (more felsic) rocks tend to form. The second largest change in physical properties is that in vesicle-free rock density, with mafic rocks exhibiting higher values than felsic ones, here the relative difference does not exceed 50% (e.g. Murase and McBirney 1973). Other varying physical parameters such as thermal conductivity, heat capacity, thermal expansion coefficient α, Young's modulus E and the Poisson ratio ν do not exhibit important variations or clear trends with composition.

There are two physical properties that do not depend primarily on major-element composition, and their importance is therefore difficult to estimate. One is the tensile strength of a rock, which is the stress that a material can withstand in extension before mechanical failure. At a given stress level, higher tensile stress will yield fewer fractures per unit distance and will therefore cause larger columns. Published values of unfractured basalt range from 8.6 to 14.5±3.3 MPa, but these studies do not address potential variations as a function of temperature, pressure or composition (Lore et al. 2000; Schultz 1995).

The other physical property is the glass transition temperature T_G, which is a second-order phase change. At this temperature, there is a change in the value of α and in the temperature dependence of E, depending on the rate of stress relaxation in the rock (Ryan and Sammis 1981). The glass transition is often defined as the temperature at which a rock has a viscosity of 10^{12} Pa s (Zarzycki 1982; Giordano et al. 2008), but its dependence on the chemical composition is complex. While the silica and alkali contents compete in controlling viscosity and hence T_G, the water content of the lava has a more important control on the glass transition temperature, with higher water content lowering T_G (Giordano et al. 2008). Water content was not systematically determined for all rocks studied here. Since the analysis of spherulite crystallisation shows low (~0.2 wt.%) water content in sub-aerially erupted felsic rocks (Castro et al. 2008) and solubility laws for water in rhyolites also result in low proportions at low pressure for extrusive lavas (e.g. Jaupart and Allègre 1991), we consider water content to be low. For intrusive felsic systems, where water content may reach higher values, the effects of more water and more silica in changing T_G are opposite (Dingwell 1996) and tend to cancel out. Therefore, we will not further discuss the effect of water content on the glass transition temperature.

Chemical composition affects physical properties mostly through the melt structure (Dingwell 1995). Structural parameters, like number of non-bridging oxygens per tetrahedron (NBO/T; Mysen 1988), are often used for such problems because they integrate the effect of melt composition on the melt structure. Therefore, we will also use NBO/T as a proxy for composition in the discussion.
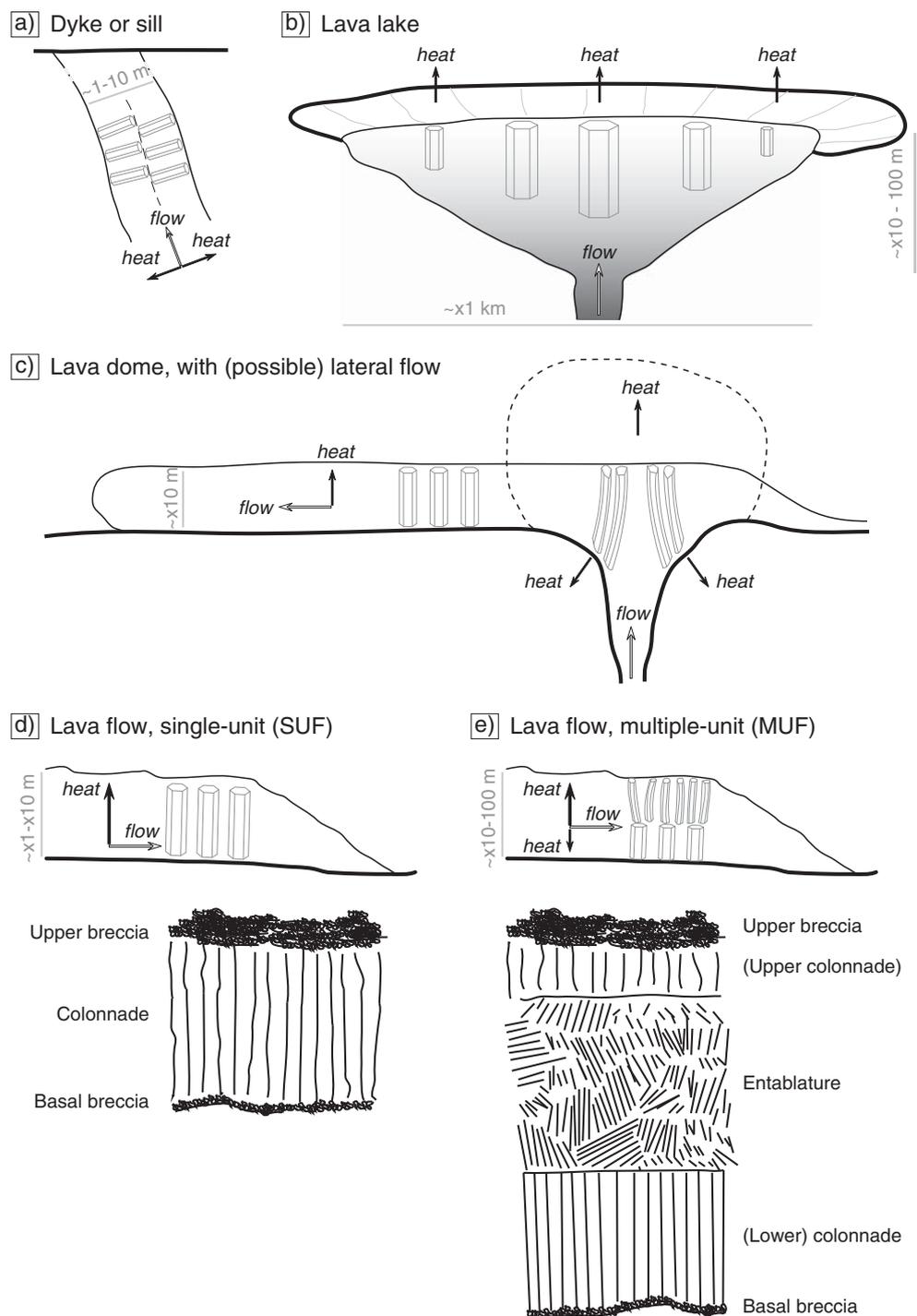
Geometry of cooling magma bodies

Geological setting

Whether magma solidifies at or below the surface controls its cooling, as heat transfer to air is much more efficient than into dry host rock. Intrusions, such as dykes, sills, laccoliths and lopoliths, are named according to their shape and size. From the columnar jointing perspective, a common problem is that the initial geometry of the intrusions is incompletely known, so the boundary conditions of the related cooling problem are not (well) known. Exceptions include planar structures such as dykes (Fig. 2a) and sills, with a double column system merging at a central line, so that their characteristic thickness can be measured. We note that from the perspective of cooling, the deeper parts of extrusive bodies (e.g. volcanic necks, narrow fissures reaching the surface) are closer to the cooling regime of intrusions, and we will classify them as "sub-surface" solidified bodies.

Extrusive bodies are usually also named after their shape at solidification: dome, flow, lake etc. Lava domes (Fig. 2c) are formed by relatively viscous, generally felsic magmas that solidify above or near the extrusion point, possibly with some lateral flow. Lava flows (Fig. 2d, e) are planar and thin relative to the area covered. Their thickness varies with palaeotopography; in the Massif Central (Mergoil and Boivin 1993), "plateau" flows are inferred to have advanced without meeting any obstacle and have a roughly constant thickness (~few 10 m), and "valley" flows fill some sort of palaeovalley or trough and hence have variable thickness (often much thicker than "plateau flows"). We follow Long and Wood (1986) in recognizing single-unit flows (SUF) (Fig. 2d, type I of Long and Wood 1986) with only one set of columns throughout the entire thickness of the flow, for which cooling is expected to have occurred dominantly from the upper surface. Multiple-unit flows (MUF) (Fig. 2e, type III of Long and Wood 1986) have at least two units, a lower "colonnade" and an upper "entablature" (see below) separated by a very sharp boundary. While the thickness of a SUF is generally smaller than that of a MUF and while there is a correlation of SUFs with "plateau" and MUFs with "valley" groups, there is no general rule to distinguish them solely upon thickness. Lava lakes (Fig. 2b) are extrusive bodies with a larger height/length ratio and can be considered as an extreme case of "valley flows". They are a consequence of lava ponding, either in craters, calderas or dammed valleys. Their thickness may reflect the palaeotopography, but this is generally hard to reconstruct. From a cooling perspective, a maar crater subsequently filled with lava is equivalent to a lava lake: a topography-confined lava body with substantial thickness variation.

Fig. 2 Schematic drawings of the different geological contexts and geometries of columnar jointing: dyke (**a**), lava lake (**b**), dome with an eventual associated flow (**c**; redrawn after Varet's (1971) example on Milhac) and lava flow (**d** and **e**; with the internal architecture after Long and Wood 1986). Note the different scales of each figure. The main direction of lava movement, as well as that of heat evacuation from the system, is indicated by *arrows*. The *hexagonal columns* schematically show the orientation and size of columnar jointing

a) Dyke or sill
b) Lava lake
c) Lava dome, with (possible) lateral flow
d) Lava flow, single-unit (SUF)
e) Lava flow, multiple-unit (MUF)

heat *heat* *heat* *heat* *flow* *heat* *flow* *heat* *flow* *heat* *heat* *heat* *flow* *flow*

~1-10 m ~x10 - 100 m ~x1 km ~x10 m ~x1-x10 m ~x10-100 m

Upper breccia
Colonnade
Basal breccia

Upper breccia
(Upper colonnade)
Entablature
(Lower) colonnade
Basal breccia

A note on colonnade and entablature

Colonnade and entablature are described in the literature as architectural units of columnar jointed lava flows (e.g. Budkewitsch and Robin 1994). Colonnade is a single range of columns in the lower part of the body, where individual columns can be followed continuously from the lower surface to a sub-planar upper boundary, with their axes roughly perpendicular to both. Colonnades are generally interpreted as the result of regular cooling in the lower part of a planar-based lava flow. Entablature, in contrast, designates a more disordered set of columns, often fanning, curving and terminating against each other. The entablature is usually located in the upper part of a solidified lava flow and exhibits narrower columns. According to one interpretation (e.g. DeGraff and Aydin 1987; DeGraff et al. 1989), the entablature does not form in a simple conductive manner, but with additional water (from heavy rains, floods

from reservoirs dammed by the flow itself (Saemundsson 1970; Long and Wood 1986)) or ice (glacier bounded or high altitude snow covered surfaces (Spörli and Rowland 2006)) that significantly accelerates the cooling to cause slender columns and by infiltrating into cracks to form new cooling surfaces, inducing the irregular pattern (Long and Wood 1986). Some flows also include a third pseudo-columnar zone made of short, large, rough columns on top of the entablature (e.g. Long and Wood 1986), but it is not often observed since it is thin and it is generally the first zone removed by erosion.

The terms "colonnade" and "entablature" derive from field observations of mostly basaltic columns and are characteristic of MUF (Mergoil and Boivin 1993). Our study addressed a wide range of compositions and emplacement types, but only seven of our columnar jointing sites exhibit a colonnade-and-entablature structure (St-Flour, Chilhac, St-Arcons, Prades, Edembouches, Bagó-kő and Dverghamrar). In order to consistently compare our columnar jointing sites in terms of conductive cooling, we measured only the geometries of joints in the colonnades and do not discuss the entablatures. For all investigated sites, columns are mostly continuous throughout the entire unit: Recombination of two columns into one (or, conversely, bifurcation of a column) is rare. Therefore, the use of a single parameter (mean side length L) to characterise the size of columns is appropriate (Characterisation of the joint-bounded columns Section).

Size of the solidified magma body

The dimension of the solidified magma body which governs the cooling process is the distance (thickness) perpendicular to its largest surface, across which most of the heat is lost. For dykes, sills and widespread lava flows, this corresponds to their thickness. For other intrusive bodies, domes, valley-filling lavas, lava lakes and sub-surface magmas, this depends on their initial shape.

Unfortunately, the initial geometry of the solidified bodies may be hard to determine because of erosion and/or mining. The initial size of the body is the least well-determined parameter in our study, but we have made measurements in the field that constrain our minimum estimates.

In order to compare the cooling rates of planar extrusive (lava flow) and intrusive (dyke) bodies, we investigate in "Appendix" the simple cooling scenario of an intrusive and an extrusive lava body, and we look for their thickness at which they experience the same cooling rate. We assume a 0°C surface temperature condition for the upper part of the extrusive flow (accounting for a very efficient convective and radiative surface cooling) and a conductive cooling through the base rock, whereas intrusive lava is fully cooled by conduction into the host rock substrate. Assuming that more than half of

the initial energy remains when jointing occurs (as T_G is relatively close to the solidus), we find that an intrusive lava body should be one third thinner than an extrusive one for the jointing to occur at similar cooling rates. Although we only have one well-studied dyke in our study, we take advantage of this thickness conversion factor.

Field data of columnar jointing sites: geological setting and chemistry

We have carried out fieldwork on columnar jointed igneous bodies in four regions in three European countries. Our main goal was to cover a broad compositional spectrum (mafic to felsic) and a broad range of emplacement types (extrusive, sub-surface, intrusive). The four regions are shown in Fig. 3, and in each of them, we investigated six to 12 locations, with a total of 50 sites where columnar joint geometry was separately measured (see Characterisation of the joint-bounded columns Section), together with a description of the geometry of the emplaced body (thickness) and the geological setting. The characteristics of all sites are summarized in Table 1, and basic description of the locations is given below. The chemical composition data and measurements are provided after (Chemical composition Section) and summarized in Table 2.

France

Volcanism in the French Massif Central (Fig. 3), part of the West European Rift System, started in the Palaeocene, with most volcanic activity from lower Miocene to Holocene (Michon and Merle 2001). Rocks at the 12 sites studied are alkaline intraplate ones:

–   Saint-Flour: A 25–30-m-thick Miocene basaltic flow extends across several hundred metres below the town (Goër de Hervé 1972). This is a multiple-unit valley-filling (see Chemical composition Section) flow, with a lower colonnade and an upper entablature (Goër de Hervé 1972). As for other valley-filling flows investigated, size and shape of columns have been measured in the colonnade, which has an average thickness of 8.5 m between the top of the basal breccia and the very sharp colonnade/entablature transition.
–   Chilhac: At this site, a 1.6-Ma basaltic valley-filling flow captured by the Allier River (Mergoil and Boivin 1993) has a well-developed colonnade and an entablature (MUF). At the measurement site, the flow is about 25 m thick (Bout 1960), with a ~7-m-high colonnade. The lava flew on a steep slope and ponded in the palaeo-Allier River valley (Bout 1960). A few columns are curved at the base towards the slope.
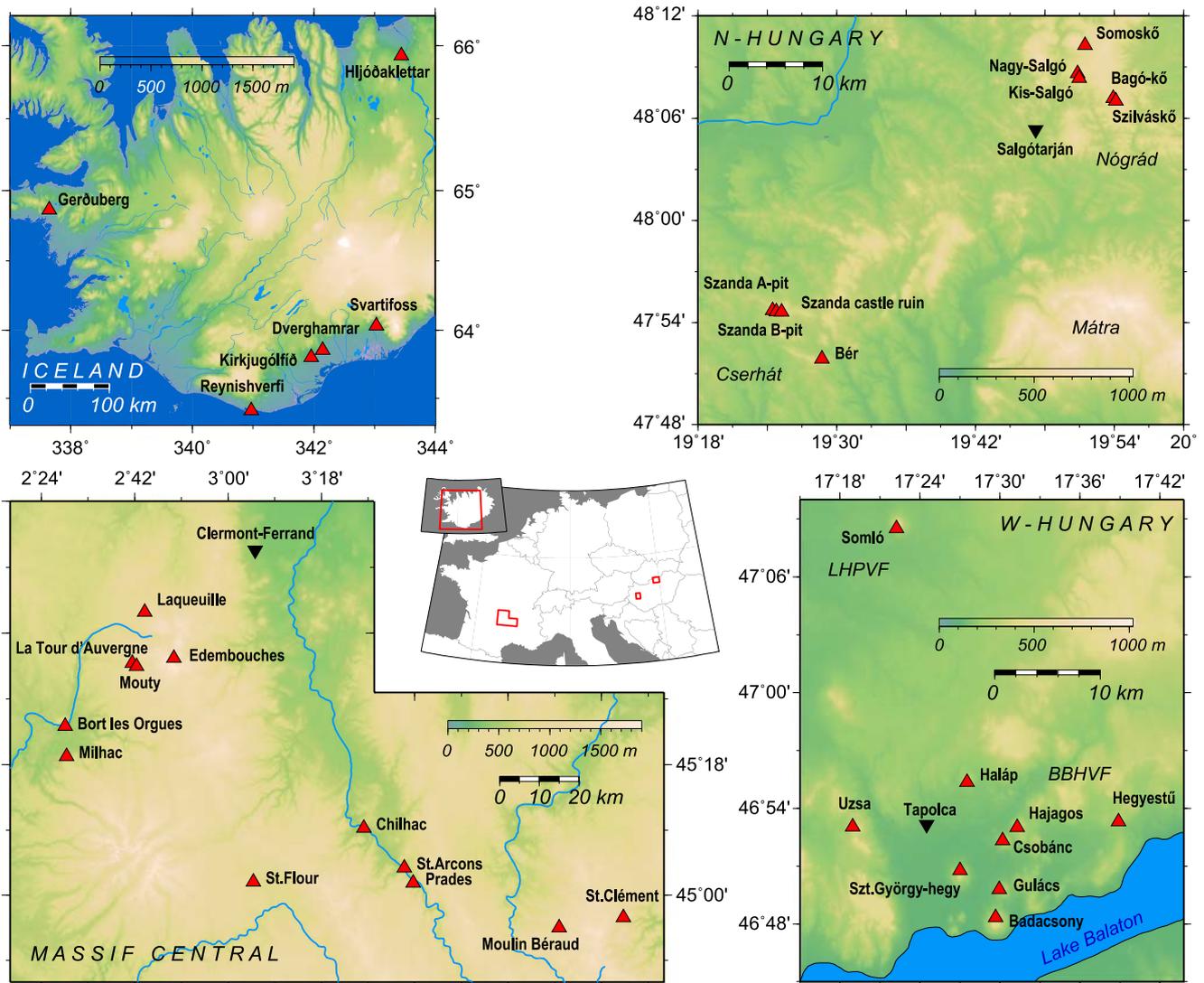
Fig. 3 Visited columnar jointed igneous rocks in Europe (*middle*, with *inset*), with *boxes* corresponding to the more detailed maps of Iceland (*top left*), of the Massif Central in France (*bottom left*) as well as of western (*bottom right*) and northern (*top right*) Hungary. Volcanic fields and regions mentioned in the text are shown. The full list of sites (*red triangles*) with coordinates is given in Table 1 and can be readily visualized using Google Earth® with the electronic supplement .kmz-file. *Black inverted triangles* show neighbouring towns for reference

- Saint-Arcons: A series of four basaltic MUF (valley flows) (2.8 to 0.6 Ma) was captured in the Allier River valley (Mergoil and Boivin 1993), with lavas showing colonnade and entablature jointing. Measurements are for the thickest flow (number 3, at least 30 m thick; Bout 1960). The flow is locally irregular above the pre-existing topography (producing curved columns) and is only partly exposed at the measurement site; therefore, it could be locally thicker than reported in the literature.

- Prades: This site in the upper Allier River valley exposes one of the many basaltic MUFs that form the Devès plateau. Those flows have a very homogeneous basaltic composition, and no differentiated unit has been found, despite numerous bulk rock analyses (Mergoil and Boivin 1993). Although Prades lava has

not been analysed due to the presence of numerous mantle xenocrysts, it has the same texture and mineral-ogy as the neighbouring flows (Chilhac and St-Arcons); we therefore assume a similar basaltic chemistry. This MUF was ponded in an ancient maar crater (Mergoil and Boivin 1993), reaching 100 m thickness locally, with one colonnade and a thick, chaotic entablature.

- Saint-Clément: At this site, 12 successive basaltic to trachy-andesitic sheet-like SUF (Mergoil and Boivin 1993) overlie each other with very stout and ill-defined columns. There is only one characteristic column size per flow and no sign of multiple cooling units.

- Moulin-Béraud: At this site is a ~50-m-thick sub-vertical tephritic intrusion, with well-exposed columnar jointing perpendicular to the host granite (Mergoil and

Table 1 Visited and measured columnar jointing sites with names (column 1), geographical location (columns 2 and 3), mean side length at each site L (column 4), lava thickness estimates from the literature and from field measurements H (column 5) and the geological context of the emplaced lava (column 6)

Site name	Latitude	Longitude	L (cm)	H (m)	Geological setting
St-Flour	N45°01′55.6″	E03°04′56.8″	23	8.5–30	Flow (MUF)
Chilhac	N45°09′19.5″	E03°26′09.4″	18	7–17.5	Flow (MUF)
St-Arcons	N45°03′55.4″	E03°33′46.0″	15	9–30	Flow (MUF)
Prades	N45°01′47.0″	E03°35′40.5″	16	15–100	Flow (MUF)
St-Clément, flow 1	N44°56′56.1″	E04°16′22.0″	67	10–15	Flow (SUF)
St-Clément, flow −1	N44°56′59.0″	E04°16′28.2″	109	10–12	Flow (SUF)
Moulin-Béraud	N44°55′35.0″	E04°03′48.3″	14	5–6	Intrusive (dyke)
Laqueuille	N45°38′56.2″	E02°43′55.7″	127	15–20	Flow (SUF)
La Tour d'Auvergne	N45°31′59.1″	E02°41′33.3″	41	>10	Flow (SUF)
Mouty	N45°31′32.8″	E02°42′19.8″	27	>5	Flow (MUF?)
Bort-les-Orgues	N45°23′17.7″	E02°28′39.7″	338	80–100	Dome and flow
Milhac, flow	N45°19′06.6″	E02°29′06.7″	127	30–150	Flow (SUF)
Milhac, dome	N45°19′11.5″	E02°28′50.8″	48	30–150	Dome
Edembouches	N45°32′43.0″	E02°49′30.0″	53	10–50	Flow (MUF)
Nagy-Salgó	N48°08′40.9″	E19°50′50.2″	51	40–95	Lava lake
Kis-Salgó	N48°08′24.6″	E19°50′57.9″	22	–	Intrusive
Szanda mine A-pit	N47°54′45.3″	E19°24′37.9″	27	15–30	Intrusive
Szanda mine B-pit	N47°54′43.5″	E19°24′41.5″	36	>12	Intrusive
Szanda castle ruin	N47°54′39.2″	E19°25′16.4″	22	15–30	Intrusive
Bér	N47°51′55.7″	E19°28′43.7″	29	25–30	Intrusive
Bagó-kő	N48°07′13.8″	E19°53′55.0″	11	5–8	Flow (MUF)
Szilváskő	N48°07′05.2″	E19°54′08.8″	16	20–35	Intrusive
Somoskő outcrop	N48°10′18.7″	E19°51′28.6″	8	10–40	Intrusive
Somoskő castle wall	N48°10′18.4″	E19°51′26.1″	10	–	Intrusive
Hegyestű	N46°53′21.5″	E17°38′51.3″	18	>38	Intrusive
Szent-György-hegy 1	N46°50′35.5″	E17°26′32.6″	38	40–100	Lava lake
Szent-György-hegy 2	N46°50′50.0″	E17°27′00.8″	32	<100	Lava lake
Szent-György-hegy 3	N46°50′46.6″	E17°27′01.4″	92	20–100	Lava lake
Badacsony 1	N46°48′00.9″	E17°29′10.9″	97	40–80	Lava lake
Badacsony 2	N46°47′48.0″	E17°29′25.3″	88	<80	Lava lake
Badacsony 3	N46°48′23.5″	E17°29′41.1″	118	<80	Lava lake
Gulács	N46°49′49.5″	E17°30′00.3″	19	30–100	Intrusive
Haláp	N46°55′31.0″	E17°27′30.4″	29	>30	Lava lake
Hajagos, upper level	N46°53′04.3″	E17°31′16.9″	61	>15	Flow (SUF)
Hajagos, lower level	N46°52′59.0″	E17°31′09.0″	19	10–15	Intrusive
Uzsa mine b	N46°52′59.5″	E17°19′02.3″	22	–	Complex system
Uzsa mine c	N46°53′04.9″	E17°18′56.7″	42	–	(see Western Hungary Section)
Uzsa mine d	N46°53′08.2″	E17°18′58.4″	31	–	
Uzsa mine e	N46°53′07.5″	E17°18′53.3	37	–	
Uzsa mine f	N46°53′14.7″	E17°19′32.6″	14	–	
Uzsa mine g	N46°53′20.4″	E17°19′28.1″	22	–	
Uzsa mine h	N46°53′23.1″	E17°19′23.5″	27	–	
Csobánc	N46°52′22.6″	E17°30′11.6″	18	<30	Intrusive

Table 1 (continued)

Site name	Latitude	Longitude	L (cm)	H (m)	Geological setting
Somló	N47°08′32.8″	E17°22′13.9″	164	15–70	Lava lake
Dverghamrar	N63°50′57.5″	W17°51′36.4″	37	8–10	Flow (MUF)
Gerðuberg	N64°51′39.4″	W22°21′33.2″	78	>15	Flow (MUF?)
Hljóðaklettar	N65°56′06.5″	W16°32′08.9″	12	16–25	Intrusive
Kirkjugólfíð	N63°47′43.0″	W18°02′46.9″	15	>0.3	Flow (SUF?)
Reynishverfi	N63°24′09.3″	W19°02′28.6″	29	10–25	Intrusive
Svartifoss	N64°01′40.1″	W16°58′33.2″	32	15–20	Flow (SUF)

Empty lines separate sites in the Massif Central (France), northern Hungary, western Hungary and Iceland. See Fig. 3 for locations, as well as the electronic supplement .kmz-file using Google Earth. Question mark notes sites where the type of flow (SUF or MUF) is not certainly determined

SUF single-unit flow, *MUF* multiple-unit flow

Boivin 1993). A double column system solidified from a 5–6-m-wide dyke in the eastern end of the body, and the overhanging part of the outcrop was measured for geometry. The dyke described as mugearitic (Mergoil and Boivin 1993), but our chemical analyses (see Chemical composition Section and Table 2) indicate a more mafic tephritic composition.

- Laqueuille: Only a few, large columns are visible in the 2.25-Ma trachy-andesitic flow, belonging to the Mont-Dore stratovolcano (Brousse et al. 1989). According to map data (Brousse et al. 1989), the flow outcrops over at least a 2.5×3.5-km area and does not show any evidence of ponding or channelling. This information, combined with the observation of only one visible cooling unit in various outcrops, suggests it is a SUF. The upper and lower contacts of the original flow are not visible in the investigated outcrops, but map elevation data indicate that the actual thickness is less than 20 m and probably close to 15 m (Brousse et al. 1989).

- La Tour d'Auvergne: A trachy-basaltic flow with well-developed columnar jointing is exposed mostly in cross section at the village's market place and with a few standing columns visible near the village centre. Upper and lower parts of the flow are not visible, but a thickness of at least 10 m is observable in the village centre. Only one cooling unit is visible, and it is tentatively classified as a SUF. However, the map pattern showing the lava over 1.5 km length×0.2 km width (Brousse et al. 1990) suggests it could be an old valley flow.

- Mouty: A recent road-cut here exposes a set of basaltic columns, near La Tour d'Auvergne. The elongate shape of the flow (4 km long×0.5 km maximum wide, Brousse et al. 1990) is indicative of a "valley flow" (MUF), although there is no field evidence of multiple cooling units and only one unit is visible in the field.

- Bort-les-Orgues: Here a voluminous phonolitic composite dome-flow (2.5×2.5 km) is present with well-

exposed columnar jointed rock on the eastern and southern sides of the dome (Varet 1975). Vertical stout columns with wavy boundaries were measured on the southern part of the dome-flow, both at the top and at the bottom. According to detailed geometric measurements by Varet (1975), this southern part can be considered a single-unit flow that originated from the northern dome. The total thickness of the flow is at least 80 m according to outcrop elevations.

- Milhac: A phonolitic dome and associated single-unit flow were described and mapped by Varet (1967). The flow (eastern part) is characterised by a single cooling unit, up to 150 m thick, with very regular, thick columns (Varet 1967). The dome (western part) shows thinner vertical columns at the top (Varet 1967), and the bottom is not visible. The column sizes were measured separately for the flow and the dome, from the side in both cases. Both the dome and the flow belong to the same eruptive unit and have the same texture and chemical composition (Varet 1967).

- Edembouches: A trachy-andesitic MUF (valley flow) here fills a N–S palaeovalley cut in pyroclastic deposits, in turn cut by a more recent E–W valley providing very good outcrop. The flow comprises a 7-m-thick lower unit with regular columns and a thick, partly scoriaceous upper unit without any structure. The total height of the flow at the lowest point in the valley is about 50 m.

Northern Hungary

We have studied two different volcanic systems in northern Hungary (northern part of the Pannonian Basin): the Nógrád province near the Slovakian border and the Cserhát Hills to its SW (Fig. 3). Volcanoes in the Nógrád comprise post-orogenic alkaline basalts that erupted mostly in the Plio–Pleistocene, following Eocene–Miocene subduction

Table 2 Major-element composition of columnar joint forming lavas

Site name	SiO₂	Al₂O₃	Fe₂O₃	MgO	CaO	Na₂O	K₂O	TiO₂	MnO	P₂O₅	H₂O	L.o.i.	Ref.
St-Flour	46.80	17.00	12.51	5.60	8.20	3.30	2.10	1.80	0.15	0.70	3.05	–	1
Chilhac	44.51	13.70	11.56	10.44	10.75	4.49	1.26	2.57	0.18	–	0.33	–	2
St-Arcons	44.80	14.05	12.02	9.50	10.00	3.35	1.70	3.05	0.19	0.15	0.46	–	3
Prades													–ᵃ
St-Clément flow 1	47.40	17.03	11.00	3.27	8.64	4.46	2.32	2.73	0.25	1.50	–	–	3
St-Clément flow −1	54.57	18.54	7.18	1.46	5.00	5.79	3.57	1.53	0.23	0.57	–	–	3
Moulin-Béraud	44.86	16.42	12.59	3.91	9.17	4.66	2.54	3.16	0.26	1.79	–	0.66	New
Laqueuille	53.40	18.52	7.56	2.69	7.18	4.28	3.04	2.24	0.14	0.46	1.17	–	4
La Tour d'Auvergne	50.48	14.72	8.65	5.94	8.47	3.71	3.08	2.04	0.17	0.48	–	2.30	New
Mouty	42.90	14.00	12.40	11.80	11.40	3.20	1.45	3.00	0.19	–	–	–	5
Bort-les-Orgues	58.70	19.10	3.92	0.40	2.40	7.20	5.60	0.50	0.22	0.20	0.60	–	6
Milhac (flow, dome)	56.84	15.38	5.37	0.02	4.98	6.00	4.88	0.39	0.07	1.00	3.42	–	7
Edembouches	54.41	16.50	7.63	2.20	7.53	4.58	3.74	2.60	–	0.30	1.25	–	6
Nagy-Salgó	46.97	15.21	10.18	7.49	9.62	3.95	2.19	2.13	0.16	0.52	–	0.07	8
Kis-Salgó													–ᵃ
Szanda mine A-pit	56.19	17.89	8.07	3.00	8.15	2.84	2.29	1.06	0.13	0.19	–	0.50	New
Szanda mine B-pit	55.98	18.17	7.93	2.96	8.29	2.89	2.15	1.04	0.13	0.19	–	0.53	New
Szanda castle ruin													–ᵃ
Bér	55.50	16.01	7.86	5.37	8.66	2.40	2.16	1.21	0.15	0.23	–	0.69	New
Bagó-kő													–ᵃ
Szilváskő	46.74	16.80	10.90	4.90	9.46	4.57	2.57	2.01	0.21	0.60	–	1.58	8
Somoskő	45.91	16.62	10.26	5.51	9.12	5.00	2.62	1.96	0.21	0.60	–	0.36	8
Hegyestű	44.17	15.65	10.24	8.15	10.32	3.70	2.51	2.34	0.18	0.65	1.22	0.91	9
Szent-György-hegy	48.59	16.27	9.91	7.55	8.59	3.05	2.45	2.06	0.15	0.63	–	1.14	10
Badacsony	45.88	15.81	10.51	8.16	9.31	4.34	2.38	2.22	0.19	0.77	–	0.55	10
Gulács	46.73	15.69	10.46	8.23	8.99	3.54	2.33	2.15	0.16	0.77	–	1.13	10
Haláp	49.30	15.85	10.28	7.99	8.62	3.16	1.78	2.07	0.15	0.52	–	0.59	10
Hajagos	47.16	14.69	10.13	9.12	7.85	2.89	2.19	2.12	0.17	–	3.64	–	11
Uzsa mine	47.08	15.66	9.94	7.67	8.78	3.31	1.91	2.09	0.16	0.66	–	2.40	10
Csobánc	47.29	15.57	10.67	6.87	8.43	4.18	3.45	2.19	0.17	–	1.84	–	11
Somló	49.01	15.78	10.44	6.99	8.29	3.66	2.34	2.09	0.17	0.72	–	0.43	10
Dverghamrar													–ᵃ
Gerðuberg	46.88	15.53	12.85	7.51	11.07	2.90	0.71	2.41	0.22	0.44	–	–	12
Hljóðaklettar	49.72	13.82	13.85	6.85	11.89	2.44	0.24	1.67	0.20	0.12	–	–	13
Kirkjugólfíð	48.07	13.94	13.91	7.23	11.80	2.25	0.23	2.23	0.21	0.19	–	−0.48	New
Reynishverfi	46.75	13.20	16.26	5.22	10.40	4.30	0.56	4.30	0.17	0.49	–	–	14
Svartifoss													–ᵃ

Data values indicate weight percent. Empty lines separate sites in the Massif Central (France), northern Hungary, western Hungary and Iceland. See Fig. 3 and Table 1 for locations. Iron was analysed as Fe₂O₃. New measurements (six sites) were carried out on fusion discs by X-ray fluorescence (XRF). We used a standard procedure with a PANalytical Axios (PW-2450) wavelength dispersive, sequential XRF spectrometer at ETH Zürich, with a rhodium tube as the source of radiation. The weighed samples were dried at 1,050°C for 2 h (yielding the loss on ignition values), were afterwards mixed with a di-lithium tetraborate flux in a sample to flux ratio of 1:5 and then melted to produce flat glass discs

L.o.i. loss on ignition, *1* Maurizot-Blanc (1974), *2* Cheguer (1990), *3* Mergoil and Boivin (1993), *4* Brousse (1961), *5* new outcrop due to road-construction, petrographically identical to a neighbouring flow (Montagne d'Ance) analysed by Mossand (1983), *6* Brousse (1961), *7* Varet (1967), *8* Dobosi et al. (1995), *9* Kóthay (2009), *10* Embey-Isztin et al. (1993), *11* Gméling et al. (2007), *12* Jakobsson (1972), *13* Sigvaldason (1974), *14* Hemond et al. (1993)

ᵃ Description of sites without data: Prades: difficult to measure due to numerous enclaves, composition should be similar to Chilhac and St-Arcons; Kis-Salgó: composition as that of Nagy-Salgó about 500 m away; Szanda castle ruin: no fresh sample available; Bagó-kő: composition as that of Szilváskő about 1 km away and Dverghamrar and Svartifoss: no sample available

and its related calc-alkaline volcanism (Embey-Isztin et al. 1993; Dobosi et al. 1995). The Cserhát Hills are mostly built up of these earlier, mainly Miocene calc-alkaline lavas. As a consequence of these various events, one can observe within a small area both classical basaltic and rare andesitic columnar jointing sites (Tardy et al. 2009).

Among the mafic basalt sites in Nógrád, the following ones have been measured (Fig. 3):

– Nagy-Salgó (a.k.a. Salgóvár): The ruins of Salgó castle sit on top of this remnant volcanic cone of basaltic composition and Early Pliocene age (Dobosi et al. 1995). What remains today is a neck (inferred to represent the mouth of a vent) representing a former lava filled crater (Tardy et al. 2009, p. 57), exposing relatively stout columns.

– Kis-Salgó (a.k.a. Boszorkánykő and Rock of Fakó Pál): The neighbouring hill to Nagy-Salgó exposes a lava body that filled a fissure created by an earlier phase of the volcanism. The lava solidified sub-surface in the fissure; its remnant is relatively small (a few 10 m wide and ~10 m thick). The rock has spalled layers on the edges, with only small areas of columnar jointing. It is proposed that the fissure originated from Nagy-Salgó and that the composition and age of the lava should be similar (Tardy et al. 2009, p. 57).

– Szilváskő: Here Pliocene basalt lava (Dobosi et al. 1995) solidified sub-surface by filling a volcanic fissure (Tardy et al. 2009, p. 58) and was later exposed due to coal mining in the area. The total thickness of the basalt is 20–35 m, and the lower two thirds of the outcrop were accessible to measure column geometry.

– Bagó-kő: This location near Szilváskő is thought to be a lava flow filling up an erosion channel (Tardy et al. 2009, p. 58). The outcrop exposes two levels of jointing: a slightly thicker row of columns standing vertically at the bottom and a set of more slender and disorganised columns on top, whose axis is sub-horizontal. The total thickness is 5–8 m, but because of the two distinct set of columns, it can still be qualified as a MUF similar to the much thicker examples in the Massif Central.

– Somoskő (in Hungarian and Šomoška in Slovak): This is a well-known site of columnar jointed basalt, on the Slovak–Hungarian border, on which sits the castle of the same name. An inferred maar-like volcano dated to the Early Pliocene has been strongly eroded. The outcrop exposes the neck under the former crater of the maar. The neck (or its transition to the base of the crater) is ~160 m in diameter and asymmetric; its eastern side was measured for geometry where the slender columns are curved. This outcrop is exposed due to the construction work of the castle in the thirteenth–fourteenth century, and excavated basalt columns are prominent in cross section and have been measured where exposed in the fortification wall (Tardy et al. 2009, p. 58; information board at the outcrop).

In the Cserhát Hills, only remnants of volcanic edifices are visible (Fig. 3). Intrusive bodies that have solidified at depth along "fissures" (with no connection to the surface) are well-preserved and outcrop mostly because they have resisted erosion better than have softer surrounding sediments (e.g. Juhász 1987).

– Szanda: Szanda-hegy is a mountain with two peaks south of the village of Szanda. The pyroxene-andesite magma forming this mountain solidified at depth within a vent (Tardy et al. 2009, p. 48) and is partly exposed in a quarry. We have measured three sites of this vent: (1) one in the mine's (western) "A-pit", on top of the western summit; (2) one in the mine's (eastern) "B-pit", one mining level below and on the northern side of the mine road and (3) one set of straight columns plunging at ~75°, immediately below and south of the castle ruin on the eastern summit (see electronic supplement Google Earth .kmz-file for precise locations).

– Bér: The site at Nagy-hegy was part of a several kilometre long fissure volcano with exposure in a quarry of rocks having solidified at depth (Prakfalvi 2002; Tardy et al. 2009, p. 49). The andesite columns here have a rare curved axis, which is due to the geometry of the intrusion, over which a set of sub-horizontal columns are displaced by tectonic movements Prakfalvi (2002).

Western Hungary

Sites visited in western Hungary are alkali basalts of the Bakony–Balaton Highland Volcanic Field (BBHVF), and we also visited one site in the Little Hungarian Plain Volcanic Field (LHPVF; Harangi et al. 1995) (Fig. 3). The BBHVF includes around 100 eruption centres (e.g. Nemeth and Martin 1998; Martin et al. 2002) and was active from the Late Miocene to the Pleistocene (Wijbrans et al. 2007; Kereszturi et al. 2011). As the syn-volcanic palaeosurface was higher than it is today, currently visible edifices correspond to both former intrusive bodies as well as preserved maars, scoria cones and lava fields (Martin and Németh 2004). Only the largest lava bodies were big enough to resist erosion and maintain a well-preserved edifice (Martin and Németh 2004). Visited sites are described in the following:

– Hegyestű: This site is a remnant plug of a volcanic conduit (Nemeth and Martin 1998; Martin and Németh 2004, p. 83; Kereszturi et al. 2011). Although its origin is still not fully established (K. Németh, personal communication, 2011), the currently exposed parts of the lava body solidified sub-surface. Hegyestű is exposed and cut in half due to mining in the past; we

have measured columnar joint geometry at the lowest level of the former quarry.

– Szent-György-hegy: This is one of the largest volcanic edifices preserved in the BBHVF, with a diameter of ~1 km and an estimated thickness of up to 100 m. In the literature, it is described as a "maar/scoria cone/lava lake" (Nemeth and Martin 1998; Kereszturi et al. 2011) and as a "multiple volcanic complex" (Martin and Németh 2004, p. 33). We interpret the lava lake part as a thick lava body with variable (currently not reconstructed) thickness. We have measured columnar joint geometry: (1) at the western parking lot, (2) near the place called Ice-Cave (north side of the hill) and (3) at the well-known, large and tall Basalt Organs (northeast side) (see electronic supplement Google Earth .kmz-file for precise locations).

– Badacsony: This is an edifice similar to Szent-György-hegy both in its appearance and origin, also considered as the remnant of a "maar/scoria cone/lava lake" (e.g. Juhász 1987; Nemeth and Martin 1998). Its diameter is ~1 km and its thickness estimated at up to 80 m. We have measured columnar joints: (1) above the place called Rodostó (west side of the hill), (2) at the Ranolder Cross (south side of the hill) and (3) at the Kőkapu (north side of the hill) (see electronic supplement Google Earth .kmz-file for precise locations).

– Gulács: This volcanic cone has a relatively regular shape and is described as a "maar/scoria cone/lava lake" (Nemeth and Martin 1998) or maar (Kereszturi et al. 2011). The rocks cropping out on its western side, well below the current topographic high, expose deeper parts that would have solidified far below the cooled upper surface. Access to most rock columns is difficult, so we acquired measurements in a former pit at the northwestern side of the hill.

– Haláp: This is a relatively large (~0.5 km diameter) volcanic edifice (Martin and Németh 2004, p. 33) where a maar (and eventually scoria cone) created in an initial volcanic phase was filled by a lava lake (Nemeth and Martin 1998; Kereszturi et al. 2011). Extensive mining has removed most former relief of Haláp, and exposed rocks are inferred to represent the middle-to-bottom part of the lava lake and its contact with the former crater (Martin and Németh 2004, p. 84).

– Hajagos: This edifice like Haláp is a maar/tuff crater subsequently filled with up to three basanite lava flows with individual thicknesses up to 10 m (Martin and Németh 2007). The quarry currently exposes (1) larger upper columns corresponding to one of the lava flows and (2) thinner columns at the quarry's lower level, representing the feeder vent of the crater zone (Martin and Németh 2007).

– Uzsa: This site is the largest Pliocene volcanic remnant in the western BBHVF. Here a lava capped mesa is composed of multiple sub-horizontal flow units (Martin and Németh 2004, pp. 134–135; Németh and Martin 2007). The internal architecture of Uzsa is revealed by an active quarry, but we cannot confidently associate this site to a geological setting category. In the quarry, we measured columnar jointing at seven sites: in the western pit's middle (b) and lower level (c south wall, d east wall, e west wall) and in the eastern pit's upper (f) and lower level (g east wall, h north wall).

– Csobánc: This remnant, referred to as a maar (Kereszturi et al. 2011) or a "maar/scoria cone/lava lake" suite (Nemeth and Martin 1998), is cut by basanite feeder dykes (Martin and Németh 2004, p. 88) on the northwest; these are columnar jointed, though the geometry of the dykes cannot be inferred.

– Somló: This butte in the LHPVF (north of the BBHVF; Fig. 3) is ~1 km in diameter and is capped by lava about 70 m thick (Martin and Németh 2004, p. 166). The internal structure of the edifice is unclear, and both a thick lava flow and a lava lake (as at Badacsony and Szent-György-hegy of similar appearance) have been inferred. The measured columns are located on the southern side of the hill and are ~15 m high.

Iceland

Volcanism in Iceland has been ongoing since at least 15 Ma (Hardarson et al. 1997; Saemundsson 1986) and interpreted to be the result of a hotspot juxtaposed with the Mid-Atlantic Ridge (Vink 1984). The lavas investigated here are all of basaltic composition (alkali-basaltic to tholeiitic) and their ages span from Tertiary to present. The visited columnar jointing sites are the following:

– Dverghamrar: Exposed here is a lava flow with a well-developed lower colonnade and parts of the entablature (MUF). The area is dominated by an alternating near-horizontal succession of lava flows interbedded with pyroclastic material, exposed in ~200-m-high cliff walls north of the outcrop. The total thickness of the exposed section is approximately 8–10 m with upper colonnades 3–4 m in length.

– Gerðuberg: Columns here have formed in a flat-lying, voluminous sub-aerial lava flow (Guillou et al. 2010) near the base of the Snæfellsnes Peninsula in western Iceland. Most rocks in this area are alkali-basaltic ones (Sigmarsson 2007), and Gerðuberg rocks probably have a similar chemistry. A well-developed colonnade (up to 15 m high) is exposed for ~200 m along the road. The mapped aerial extent of this lava flow is about 2 km in length by 0.4 km in width, suggesting a topographically confined lava flow. Contacts are

unexposed in the field, however, so it is difficult to establish whether this is a MUF as are most ponded flows in the Massif Central, or a SUF.

– Hljóðaklettar: Columnar jointing at this site is highly irregular, and the locally chaotic arrangement of the columns is probably a result of sub-surface solidification of an irregularly shaped intrusion injected into wet sediments. This interpretation is based on the strong resemblance in the arrangement of the columns to those observed at Reynishverfi (where the contacts are preserved). However, no contacts to the surroundings can be observed so the exact mode of emplacement is difficult to determine.

– Kirkjugólfíð: Rocks here are tholeiitic (Thorarinsson 1981), exposed in an outcrop measuring approximately 80 m^2. They are of columnar jointed basalts that can be viewed from above (i.e. in cross section). Thickness of the exposed section is approximately 0.3 m with no direct contacts to the surrounding lava flows observed. At the base of the exposed section is a horizon with irregularly developed jointing. It is, however, impossible to say if this is the disturbed base of the lava flow or if it represents the entablature (and the exposed columnar jointing corresponds to the lower part of the upper colonnade); therefore, we classify this site as a potential single-unit flow.

– Reynishverfi: At this marine erosion has exposed columnar jointed basalt and palagonite breccias. The outcrop is approximately 160 m high, and columnar jointing can be found at different levels within it. Overall the orientation of the jointing is highly irregular, but joints are systematically arranged towards the central parts of the intrusion, and we made our measurements here. At the contact to the palagonite, there are abundant peperite textures, indicating intrusion into wet sediments.

– Svartifoss: At this waterfall in the Skaftafell National Park is exposed a 20-m-thick columnar jointed lava flow with a well-developed colonnade. No contact to the surrounding topography is exposed at this location, and no entablature can be observed. However, the arrangement of the columns is slightly more disturbed on the western side of the outcrop. Based on the flat character of the exposed outcrop, which is in agreement with the overall topography of the surroundings, it is interpreted as a simple lava flow.

Chemical composition

Data on major-element composition of the majority of rocks studied are available from the literature (Table 2). For 12 sites lacking such information, we:

– Carried out new major-element compositional analyses for samples from six locations (see below)

– Used data from nearby lavas of the same mineralogy and similar age at three locations (Prades, Kis-Salgó, Bagó-kő)

– Proceeded without compositional data for three sites in absence of available fresh samples (Szanda castle, Dverghamrar, Svartifoss)

The rocks analysed range from tephrite–basanite to trachyte and phonolite (Fig. 4). Most rocks of our study are basanites and trachy-basalts (i.e. basalts *sensu lato*). The small range in composition seen for three of our sites (Hegyestű, Badacsony, Szent-György-hegy) does not influence our results.

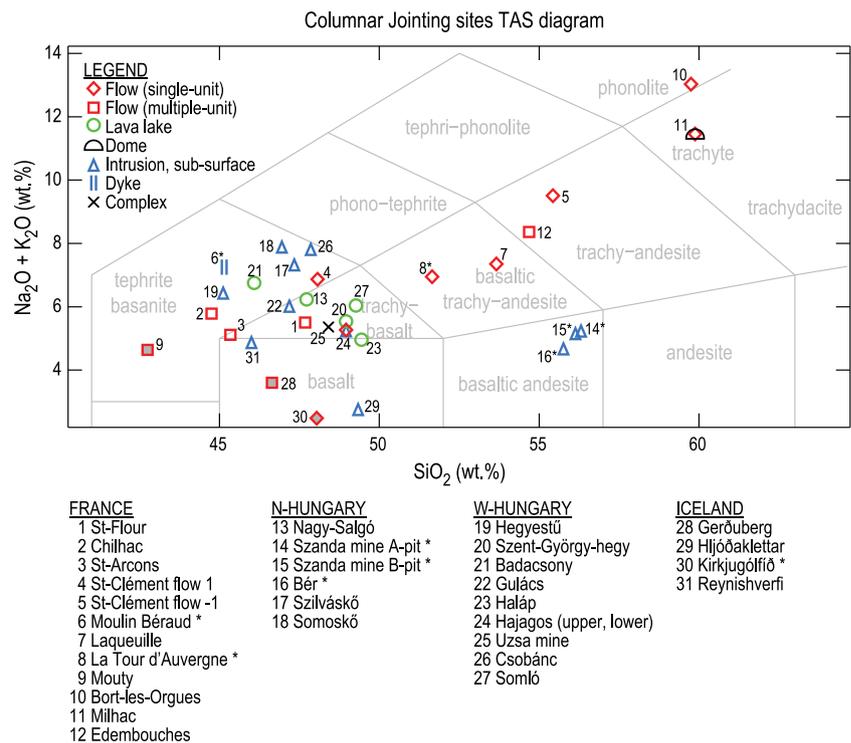## Characterisation of the joint-bounded columns

Measuring column geometry

Parameters defining column size

We describe the geometry of columnar joints from scaled outcrop photos, then process the information using a MatLab® routine (Characterisation of column geometry: results and discussion Section). We distinguish between two different types of views when taking photographs: views perpendicular to the columns (Fig. 5a) and views from the side of the columns (Fig. 5b). In perpendicular view, one can measure the length of each column-bounding joint L, the area of each column in cross section A and the order of the polygon N defining each column (Fig. 5c). In side view, one can measure the apparent distance between fractures that bound the columns vertically (L) and add additional information for the profile width of columns with two ($D2$) or three ($D3$) joint faces exposed (Fig. 5d). The apparent distances $D2$ and $D3$ have to be converted to a measure of L by taking the $D2/L$ and $D3/L$ ratios of columns seen perpendicularly (Fig. 5e) in order to integrate these measures in statistics on side length (Characterisation of column geometry: results and discussion Section). Finally, the side view also allows measurement of the exposed thickness of the magma body H; this is only a minimum estimate as the extent of the lava beneath the surface and to the amount of eroded material is unknown (see discussion in Geometry of cooling magma bodies Section).

Processing software

We have developed an interactive software package using MatLab® (from MathWorks Inc.) to process the photographs taken in the field. After reading an image, a linear scaling is performed calibrated to the scale used in the field. We do not correct for optical distortion of images because the photos were taken from a distance.

Fig. 4 Compositional variability of investigated columnar jointed igneous rocks, as shown on a total alkali–silica diagram. *Symbols* according geological setting; *flow symbols* with *grey fill* correspond to sites where the flow type could not be established certainly. *Stars* behind site names stand for compositions determined by this study. For the full major-element composition of rocks, see Table 2

Columnar Jointing sites TAS diagram

LEGEND
◇ Flow (single-unit)
☐ Flow (multiple-unit)
○ Lava lake
⌂ Dome
△ Intrusion, sub-surface
‖ Dyke
✕ Complex

FRANCE	N-HUNGARY	W-HUNGARY	ICELAND
1 St-Flour	13 Nagy-Salgó	19 Hegyestű	28 Gerðuberg
2 Chilhac	14 Szanda mine A-pit *	20 Szent-György-hegy	29 Hljóðaklettar
3 St-Arcons	15 Szanda mine B-pit *	21 Badacsony	30 Kirkjugólfið *
4 St-Clément flow 1	16 Bér *	22 Gulács	31 Reynishverfi
5 St-Clément flow -1	17 Szilváskő	23 Haláp	
6 Moulin Béraud *	18 Somoskő	24 Hajagos (upper, lower)	
7 Laqueuille		25 Uzsa mine	
8 La Tour d'Auvergne *		26 Csobánc	
9 Mouty		27 Somló	
10 Bort-les-Orgues			
11 Milhac			
12 Edembouches			

The scaled photograph is then processed using one of the following options:

– Side view: The user locates (i.e. manually clicks the position of) the fractures that vertically bound the columns and enters the number of visible sides for each column. The software saves the corresponding lengths (L, $D2$ and $D3$).

– Perpendicular view: The user locates (manually clicks) all corners of a column's cross section. The software draws straight column borders and saves the length of each side L, the area of the closed polygon A and polygon order N and computes $D2$ and $D3$, assuming consistent column polygonality, for later conversion of side view measurements. When a column is not entirely visible on the photograph, only the length information for visible borders is saved.

– Semi-automatic clicking: This mode is useful when a larger number of packed columns are visible in cross section (Fig. 6). Here, by first manually clicking all vertices (joint junctions) and then entering (from the keyboard) the order of each polygon, considerable time is saved (a short description of this mode can be found in the legend of Fig. 6b). In this mode, the software saves the same parameters as in perpendicular view.

The information is saved and processed to create statistics. The conversion of $D2$ and $D3$ to L allows combining the length measurements from perpendicular and side views. The collected information on L, A and N provides the distribution of each parameter and allows determination of their mean value and range of variation.

Sources of uncertainty

Several sources of potential error can be identified. Deviation from perpendicular when taking a photograph causes 0.4% error at a 5° deviation and 1.5% error at 10°. Distortion due to the camera's optics is estimated to be lower. To account for these technical uncertainties, we round all length estimates to the closest centimetre, which we consider as a reasonable lowest error estimate on measured distances.

Other uncertainties arise from practical difficulties. The boundary separating columns can be curvilinear or simply hard to detect. We have observed dividing/merging columns, as well as very large and ill-defined columns. To avoid artefacts from the interpretation of these structures, we excluded information from these situations. Another practical source of uncertainty is the software user effect: The way and precision of clicking vary from one person to another. To assess such variations, we performed a clicking test with four users on a single drawing of joint patterns from the Giant's Causeway shown in Fig. 6a, using the software's semi-automatic mode (Table 3). Although there is a difference in the number of columns clicked, which we interpret as resulting from the poor quality of the drawing

Fig. 5 Characteristic geometrical properties measured on columnar jointed igneous rock outcrops. Field examples (a, b; at Somoskő outcrop) and corresponding measurable parameters (c, d) of perpendicular (a, c) and side (b, d) views. The side of the square-scale is 40 cm long. A is the area of the column in cross section, L is the length of a polygon side, N is the order of the polygon and D2 and D3 are the apparent distances between two or three edges of the column in side view. The conversion of D2 and D3 into a measure of L is based on the D2/L and D3/L ratios of columns measured in perpendicular view (e)
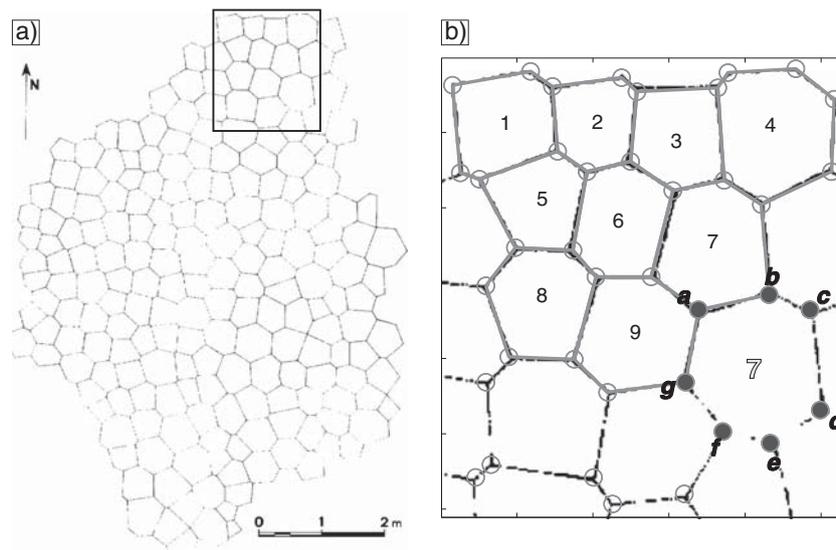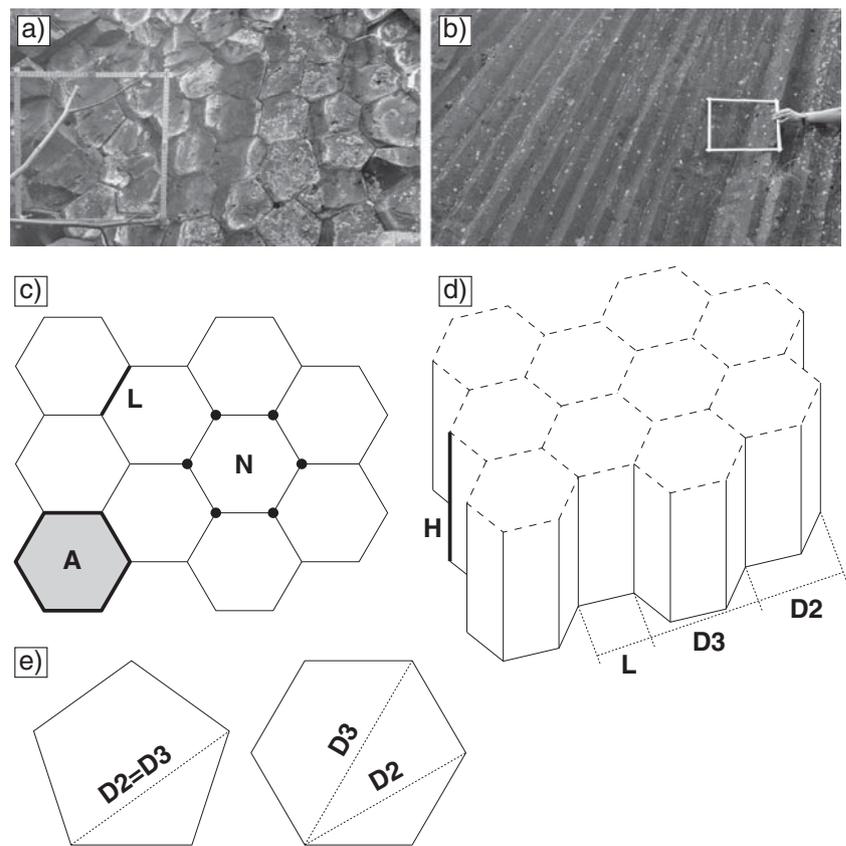
Fig. 6 a An example of perpendicular view drawn after measurements at the Giant's Causeway (from O'Reilly, 1879, redrawn in Budkewitsch and Robin 1994, p. 226). b Zoom of the rectangle in a, showing the functioning of the software developed for characterising columnar joints. Workflow of the semi-automatic mode shown here: In a first phase, the vertices are clicked and shown by *empty circles*. In a second phase, the user places the mouse in the *middle of a column* and enters the order of the polygon (here the bright contoured 7). The software locates the closest N vertices (*full circles*) and labels them with letters (here a to g). When the correct vertices are identified, the user moves the mouse to the next column: When typing the next number, the previous column is contoured (*thick solid line*) and numbered (in *black*). If the mouse cursor was not well centred and hence one or more vertices are mis-identified, pressing the corresponding letter will re-launch the search of nearest vertices omitting the one(s) in question. Also, if the entered number of vertices was wrong, pressing + or − will search for one vertex more or one vertex less. This way the semi-automatic mode avoids re-clicking the same vertices three times for the three neighbouring columns, therefore yielding higher accuracy and saving 30–50% clicking and time

Table 3 Statistics resulting from clicking the drawing in Fig. 6a by different users of the software

User	Length±1σ (cm)	#L	Area±1σ (1,000 cm^2)	#A	Number of 4/5/6/7/8-sided polygons	Average N
Beta	26±10	1,224	1.76±0.61	199	4/14/134/42/5	6.15
Epsilon	27±10	1,167	1.79±0.50	196	6/43/105/38/4	5.95
Phi 1st	27±9	1,030	1.74±0.47	174	6/40/93/32/3	5.92
Phi 2nd	27±10	1,119	1.73±0.50	189	6/43/104/32/4	5.92
Gamma 1st	27±10	1,182	1.79±0.50	198	6/44/103/40/5	5.97
Gamma 2nd	26±9	1,183	1.73±0.48	198	5/44/105/39/5	5.97

#L number of L measurement, #A number of A measurement

taken from a scanned pdf-file, the main numbers characterising the geometry agree well:

– The mean length and its 1σ range are determined within 1 cm difference (3.8% relative error).
– The area measurements are determined within a 60-cm^2 range (3.4% relative error).
– The average number of sides agrees very closely (within 1% relative error, except for the first user who took many pentagons as hexagons; when that average is included, the relative error is 3.9%).

We note that the repeatability of clicking by the same users is even better (Table 3), shown by variations smaller than mentioned above. Even though the relative user-errors are low, we processed the photographs from the field using only a small number of users: one person for the Icelandic sites, one person for the Hungarian sites and this same person shared the sites in France with a third person.

Characterisation of column geometry: results and discussion

Column sizes

Our data on the geometry of columnar joints are shown in Table 4, with mean side length data reported in Table 1 as well. Both D2 and D3 vary with the order of the polygon, which is unknown in side view, but we can reasonably define an effective conversion factor by using D2/L and D3/L ratios observed in perpendicular view, which reveals the proportion of four-, five-, six-, seven- and eight-sided polygons. This yields D2/L=1.69 and D3/L=1.85, both values lying between the ratios for pentagons and hexagons ([D2/L]$_{pentagon}$=1.62 and [D2/L]$_{hexagon}$=1.73; [D3/L]$_{pentagon}$= 1.62 and [D3/L]$_{hexagon}$=2.00), which together account for five sixths of all observed column cross sections (Fig. 7). This way, the 17,312 joint length observations from 3,033 column cross sections are combined with 6,577 joint length estimates from side views to yield a total of 23,889 joint length data.

Table 4 shows that the range of L and A varies significantly from site to site. The smallest columns have 8±3-cm-long sides on average. Most sites have columns with joint lengths below the 40±10-cm level, and some sites have very large columns, with joint lengths exceeding 3±1 m. The measured areas span at least two orders of magnitude, between 0.01 and 2.1 m^2, although the area of the columns with the longest sides could not be accurately measured.

Polygon order

The distribution of polygon order N is shown in Fig. 7. There is an overwhelming majority (83%) of hexagons (every second column) and pentagons (every third column). The mean order of polygons is less than 6 (N_{avg}=5.71), and Table 4 shows that N_{avg} is not related to the mean size of the columnar joints. The fact that N_{avg} is less than 6, for the entire dataset and also for each site with a reasonable number of observations, is unsurprising: observations from other sites described in the literature mention values between 4.87 and 5.94 (Budkewitsch and Robin 1994). It is also believed that N_{avg} tends towards but never reaches 6 as the system "matures"; that is, the network of fractures tends towards a hexagonal shape, and the angle at vertices increases with system maturity from 90° to 120° (Gray 1986; Aydin and DeGraff 1988; Budkewitsch and Robin 1994). Budkewitsch and Robin (1994) also proposed that the range of variation in cross-sectional area and the width of N-distribution should decrease in more mature systems. We have analysed the relationship between dA/A and the 1σ variation of N at different sites (Fig. 8): Apart from four outlier sites (where dA/A is large due to the non-Gaussian distribution of column sizes), there is a positive correlation. This suggests that a smaller deviation of the polygon order is intrinsically correlated to reduced variability in cross-sectional area. This strengthens the inference of Budkewitsch and Robin (1994), providing two methods to estimate the "maturity" of a columnar jointed system.

Table 4 Geometry measurements at 50 columnar jointing sites (see Fig. 3 and Table 1 for locations)

	L (cm)	$\pm \mathrm{d}L$ (cm)	#L	La (cm)	$\pm$dLa (cm)	#La	A (cm^2)	$\pm \mathrm{d}A$ (cm^2)	#A	N_{avg}
France (14)										
St-Flour	**23**	5	738	22	7	6	1,208	–	1	*6.00*
Chilhac	**18**	8	895	**16**	6	376	579	265	65	**5.78**
St-Arcons	**15**	6	847	**13**	5	408	313	112	77	**5.30**
Prades	**16**	7	420	11	4	120	263	109	21	*5.71*
St-Clément flow 1	**67**	19	141	–	–	–	–	–	–	–
St-Clément flow −1	**109**	28	28	–	–	–	–	–	–	–
Moulin-Béraud	**14**	5	1,637	**14**	5	1,637	423	152	293	**5.59**
Laqueuille	**127**	42	32	–	–	–	–	–	–	–
La Tour d'Auvergne	**41**	11	515	39	9	112	3,740	730	19	*5.89*
Mouty	**27**	7	151	23	8	12	1,256	149	2	*6.00*
Bort-les-Orgues	**338**	107	78	–	–	–	–	–	–	–
Milhac, flow	**127**	31	20	–	–	–	–	–	–	–
Milhac, dome	**48**	13	48	–	–	–	–	–	–	–
Edembouches	**53**	13	68	–	–	–	–	–	–	–
Hungary (30)										
Nagy-Salgó	**51**	16	119	–	–	–	–	–	–	–
Kis-Salgó	**22**	8	52	22	8	52	904	469	10	*5.20*
Szanda mine A-pit	**27**	9	229	**27**	9	229	1,354	544	44	**5.20**
Szanda mine B-pit	**36**	9	135	–	–	–	–	–	–	–
Szanda castle ruin	**22**	9	94	18	6	61	860	231	10	*6.10*
Bér	**29**	10	370	**29**	10	311	1,839	745	56	**5.55**
Bagó-kő	**11**	5	523	**10**	4	460	214	163	82	**5.61**
Szilváskő	**16**	7	770	**16**	5	269	549	194	48	**5.60**
Somoskő outcrop	**8**	3	1,267	**8**	3	893	144	54	156	**5.72**
Somoskő castle wall	**10**	3	1,945	**10**	3	1,892	218	69	323	**5.86**
Hegyestű	**18**	5	608	**16**	5	201	509	172	37	**5.43**
Szent-György-hegy 1	**38**	9	19	–	–	–	–	–	–	–
Szent-György-hegy 2	**32**	12	48	29	10	40	1,893	600	7	*5.71*
Szent-György-hegy 3	**92**	36	64	81	31	16	11,605	1,232	3	*5.33*
Badacsony 1	**97**	36	30	103	36	24	17,600	7,301	5	*4.80*
Badacsony 2	**88**	38	18	88	38	18	21,109	9,431	3	*6.00*
Badacsony 3	**118**	44	23	–	–	–	–	–	–	–
Gulács	**19**	5	112	–	–	–	–	–	–	–
Haláp	**29**	10	836	**27**	9	710	1,669	485	123	**5.77**
Hajagos upper level	**61**	18	98	–	–	–	–	–	–	–
Hajagos lower level	**19**	6	215	22	8	36	1,182	415	6	*6.00*
Uzsa mine b	**22**	11	269	**19**	9	202	813	596	36	**5.61**
Uzsa mine c	**42**	18	74	43	20	59	2,938	807	11	*5.37*
Uzsa mine d	**31**	6	304	–	–	–	–	–	–	–
Uzsa mine e	**37**	7	287	–	–	–	–	–	–	–
Uzsa mine f	**14**	3	69	–	–	–	–	–	–	–
Uzsa mine g	**22**	8	393	**19**	8	225	773	507	40	**5.63**
Uzsa mine h	**27**	6	143	–	–	–	–	–	–	–
Csobánc	**18**	4	12	**19**	6	5	559	–	1	*5.00*
Somló	**164**	61	32	–	–	–	–	–	–	–

Table 4 (continued)

	L (cm)	±dL (cm)	#L	La (cm)	±dLa (cm)	#La	A (cm²)	±dA (cm²)	#A	N_avg
Iceland (6)										
Dverghamrar	**37**	12	128	37	11	107	3,021	1,305	19	*5.63*
Gerðuberg	**78**	30	188	77	31	148	14,623	5,864	25	*5.92*
Hljóðaklettar	**12**	7	1,771	**12**	7	1,721	376	323	300	**5.74**
Kirkjugólfíð	**15**	5	6,186	**15**	5	6,186	530	151	1,080	**5.73**
Reynishverfi	**29**	11	808	**29**	11	744	2,046	706	125	**5.95**
Svartifoss	**32**	13	32	32	13	32	3,082	1,387	5	*6.4*
Total (50)			23,889			17,312			3,033	**5.71**

Average order of polygons (in bold/italic when more/less than 30 area measurements are available)

L mean side length, *dL* 1σ variation range, *#L* number of measurements, *A* mean area, *dA* 1σ variation range, *#A* number of measurements, appended "a" indicates the same for sides with area measurement

Polygon irregularity and energy considerations

We compare sites using the mean side length, the mean area and the order of the polygons (Fig. 9). Figure 9a shows the relationship between *A* and *L*: All sites align along a quadratic shape, which is compared to theoretical parabolae. The coefficient of a theoretical parabola relating the side length and the area of a regular polygon depends on its order *N*:

$$A = N/4 \cdot \tan(\pi/2 - \pi/N) \cdot L^2. \qquad (3)$$

The parabolae in Fig. 9a hence show the area corresponding to a given joint length if all polygons were regular pentagons or hexagons (*N*=5.5 is also shown for reference). All columnar jointing sites with a reasonable number of measurements range between *N*=5 and 6, which is in agreement with the above observations on *N*_avg. These results validate our measurement technique of the columnar joint sizes. However, one must note that since the polygonal cross section of columns is not regular, the location of a site on the *A–L* diagram does not yield exactly *N*_avg, but rather a relative position compared to regular polygons.

The shape of natural polygons compared to theoretical ones can be analysed by representing the *L–A* relationship as a function of *N* at a given site (Somoskő outcrop, Fig. 9b). The parabolic fits to data points of quadrangles, pentagons, hexagons, heptagons and octagons all lie below the theoretical curves drawn according to Eq. 3. The same trend is observed at all other sites; the parabolae fitted to
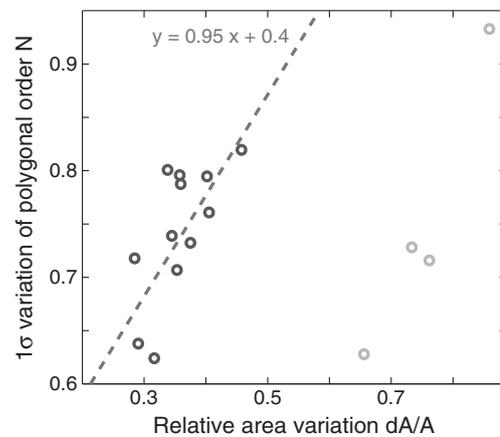

Fig. 8 Correlation between the relative area variation of column cross sections d*A/A* and the 1σ variations of the polygonal order *N* at columnar jointed igneous rock sites with more than 30 area measurements. Most sites lie along a line with a positive trend (*black circles*) and show that a narrower range of area variations implies a less dispersed distribution of column-bounding polygon order. Four sites are outliers (*grey circles*): The distribution of columns sizes is not Gaussian; therefore, the relative area error is increased and cannot be compared to the other sites
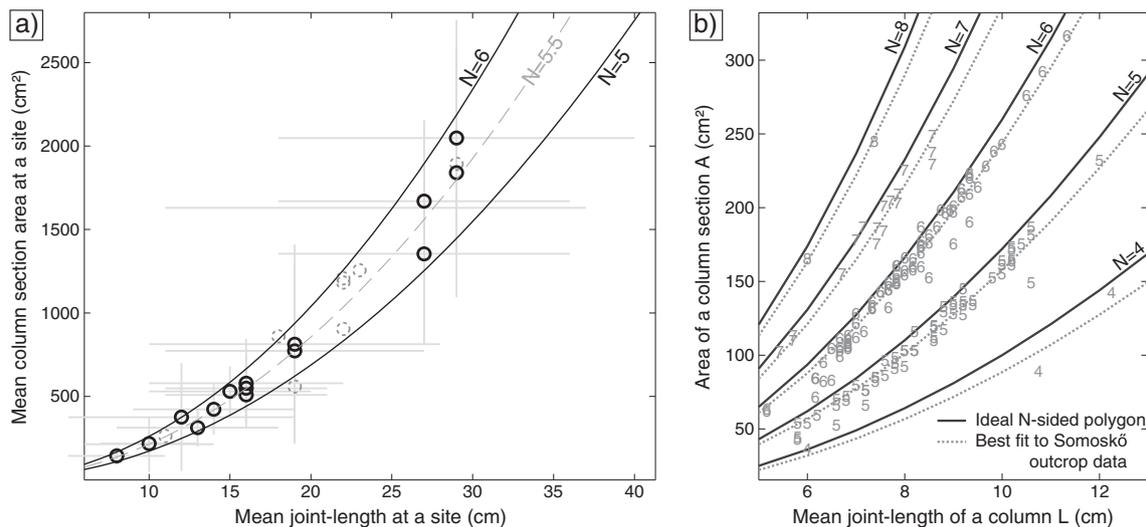

Fig. 7 Distribution of the order of the polygonal column cross sections *N* at all columnar jointing sites combined (3,033 columns). Hexagonal sections are the most frequent (every second) followed by pentagons (every third). The average order of polygons is 5.71

Fig. 9 **a** Relation of the mean side length *La* to the mean section area *A* at columnar jointed igneous rock sites. *Dashed grey circles* stand for sites with less than 30 area measurements, *solid black circles* stand for sites with more than 30 area measurements, with *grey lines* showing the 1σ variation of both *La* and *A*. Parabolae show the theoretical curves for regular hexagons and pentagons based on Eq. 3. **b** Relation

of the mean side length *La* to the mean section area *A* of the polygons separated by polygon order *N* (*numbers*) at the Somoskő outcrop site. *Solid black* parabolae show the theoretical curves for different regular *N*-order polygons; *dotted* parabolae show the best fit to the data going through the origin

data points yield an area that is on average 7% lower than the theoretical area at a given length. This area reduction appears for every polygon order *N* and is larger than the estimated error of our measurement technique.

Based on these observations, we conclude that in a columnar jointed body, the developing network of fractures defines polygons that are not regular, and the enclosed areas stay below those of regular polygons at a given side length. Conversely, from a given column-area perspective, the length of the fracture network is longer than is necessary for the creation of a regular network. Therefore, more energy is spent on creating a longer fracture network than minimally required for an ideal one. These statements stand irrespective of the column size. All these conclusions suggest that columnar jointing is a non-equilibrium process during which one or more factors (inertia of the system, inhomogeneities, environmental constraints) prevent the energy from being fully minimized.

Assessing the influence of body geometry and chemistry on columnar jointing size

Body geometry

The thickness of the studied igneous units, as said earlier, is an incompletely known parameter due to the lowering effect of erosion and/or the partial exposure of columns. With this in mind, we compare the minimum thickness of the columnar jointed body *H* and the mean side length of columns *L* at each site (Fig. 10). The data points are shown with symbols corresponding to the geological setting.

As a rough description, columnar jointing sites lie between the 100:1 and the 10:1 thickness/side length ratio. The diagram somewhat reflects our geological classification of sites, with lava lakes and domes having generally greater thicknesses than lava flows. The intrusions and bodies having solidified sub-surface seem to have relatively higher thickness/side length ratio, but their initial geometry is the least well-constrained. Within the lava flow sites, there is a rough positive trend: the thicker the flow, the stouter the columns due to slower cooling. This trend might reveal quantifiable correlation if more-precise thickness data were available; with the current limitations, this is the most we can state.

We infer that the influence of cooling body thickness on columnar joint size operates via its control of the cooling rate of a body as shown in Fig. 1. This effect is also schematically reported in Fig. 2, and it would be desirable to analyse a solidified lava lake (Fig. 2c) in detail, with good constraints on its initial geometry, to verify if the size of the columns depends on and correlates with the lava thickness. A field example indicating increased joint spacing with slower cooling is provided by Goto and McPhie (1998), who document a radially jointed dacite cryptodome, which has more widely spaced joints closer to its centre.

Chemical composition

The mean side length of columns *L* at each site is plotted against the chemical composition of the columnar jointed rock, represented by its silica content (Fig. 11a) and by its NBO/T value (Fig. 11b). The data are shown with symbols
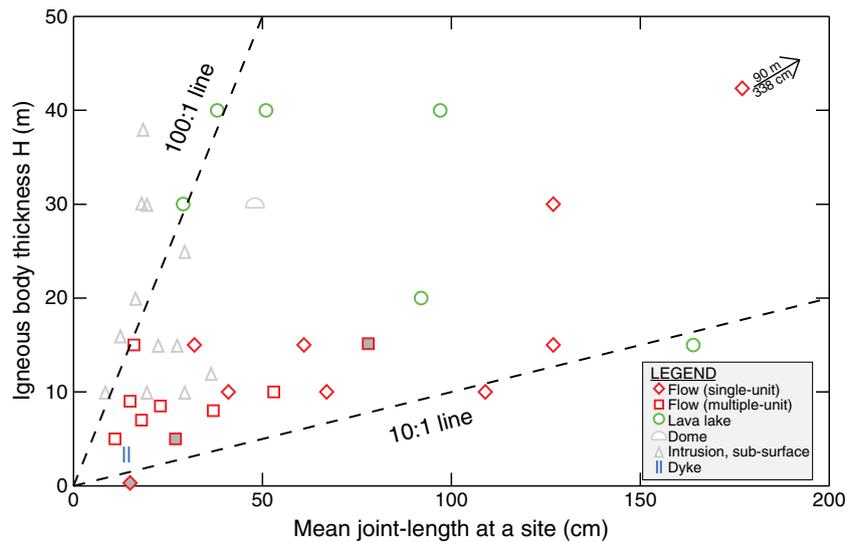
Fig. 10 Lava thickness *H* (minimum estimate) versus average side length of columns *L* at columnar jointed igneous rock sites. Since erosion and/or partial exposure may result in significantly reduced estimates of *H*, this is a very approximate view. Columnar jointing sites lie roughly within the *H/L*=100:1 to 10:1 range (*dashed lines*). *Symbols* according geological setting; *flow symbols* with *grey fill* correspond to sites where the flow type could not be established certainly. The thickness of the dyke (Moulin-Béraud site) was divided by 1.5 for reasonable comparison with free flows (see text and "Appendix")

corresponding to the geological setting, based on which the following can be stated:

– Lava lakes studied formed from mafic (SiO$_2$<50 wt.% shown in Fig. 11a) lavas only and feature columns of

all sizes, perhaps depending on the thickness of the lava

– Among studied intrusions and sub-surface solidified bodies, only slender columns are present (<40 cm side length shown in Fig. 11a), potentially due to the limited
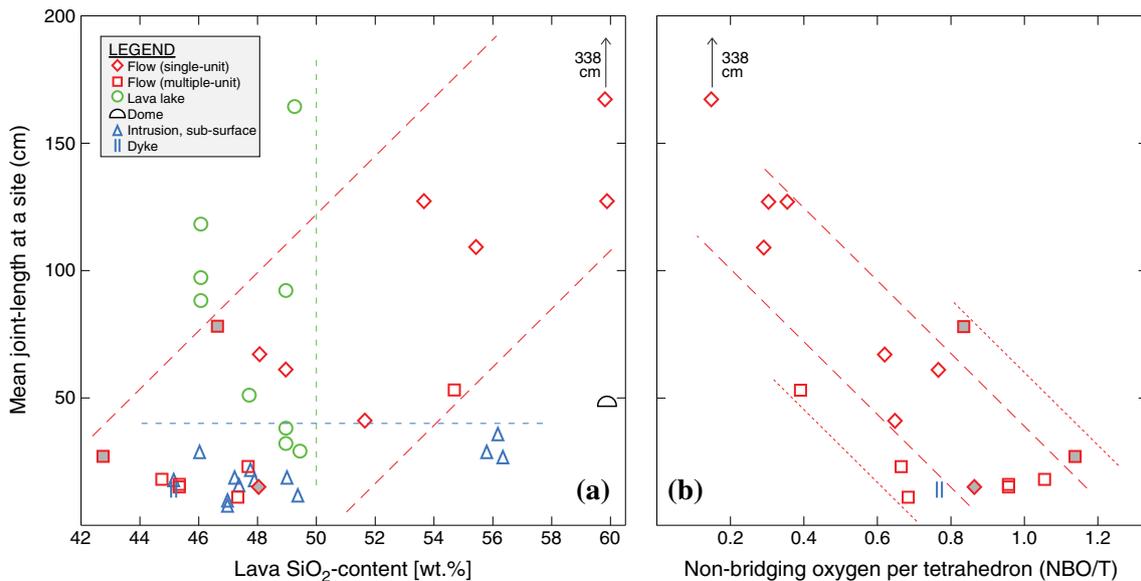
Fig. 11 Relation between mean side length of columns *L* and lava "acidity", represented by its SiO$_2$ content (**a**) and NBO/T value (**b**). *Symbols* indicate geological setting, allowing interpretation in terms of both composition and geometry of the emplaced body. *Flow symbols* with *grey fill* correspond to sites where the flow type could not be reliably established. The observed upper SiO$_2$ content limit for lava lakes in this study and the upper side length limit for intrusions and sub-surface solidified bodies are shown in *dashed lines* of the corresponding colours. The relationship between columnar jointing size and silica content in flows is indicated by *long-dashed lines*. Part **b** only shows sites with columnar jointed bodies that are associated with flows and dykes and reveals a positive correlation between lava "acidity" and characteristic column size, with roughly the same trend for single-unit and multiple-unit flows (*two different dashed lines*). See text for discussion

thickness constrained by their geometry at emplacement and to occasional contact with wet sediments. These relatively small sizes are for both mafic and intermediate compositions

– Lava flows studied show a positive correlation between SiO_2 content and column size (rough linear trends in Fig. 11a) and also a negative correlation between NBO/T and column size (Fig. 11b). The range of column side lengths is from 10 to 20 cm in mafic flows to 1.3–3.4 m in felsic flows considered. MUFs appear more common with more mafic compositions, with SUFs at more intermediate compositions, but there is a correlation between silica content and column size in both groups (Fig. 11b), including also the only planar, steep-dipping intrusion (dyke). We interpret this general correlation as indicating a primary control through the physical properties of the lava (see Proposed approach to link lava geometry and chemistry to joint spacing and Compositional control: variations in the physical properties of magma Sections)

Figure 11b only shows sites where the overall geometry of the emplaced magma body is unaffected or only slightly affected by the host environment (i.e. flows and dykes are shown, but lava lakes and sub-surface solidified bodies are not). The good correlation between the chemistry and characteristic size for this subset of magmatic bodies confirms that there is indeed an influence of chemical composition on columnar joint spacing in lavas. Felsic flows form generally larger columns than mafic flows. The correlation, however, is not straightforward, as the composition acts on column size indirectly, through three modes of control, shown in Fig. 1. The first two modes act through the mechanical and thermal properties, which, respectively, influence the stress balance and the initial conditions of cooling. The third mode of control acts through the geological setting itself: The chemistry of the lava constrains the mode of emplacement through the geological setting (Fig. 1) and also the thickness in the case of a lava flow. This is both known from field observations and visible in Figs. 3 and 11: A dome usually forms from a felsic magma, a lava lake from a mafic magma. Exceptions from the chemical control on the geometry of the emplaced body being dominant are the physically confined magma bodies (i.e. bodies having solidified sub-surface; dykes, or intrusions in general).

Lava geometry–chemistry relationships: an example

As an illustration of the relation between lava geometry and chemistry, we discuss the case of the well-known Devils Tower in Wyoming (USA). It is a phonolite body thought to be a volcanic neck. The diameter of the columns ranges between 2 and 5 m at its base and is about 1.5 m at its top (Karner and Halvorson 1989). These sizes are consistent with our observations at Bort-les-Orgues and Milhac, where columns

with 1–3-m joint lengths were observed in thick, felsic lava flows. Furthermore, the increase in column size from top to bottom calls for a downwards decreasing cooling rate; this can be explained by (1) the downwards broadening fan shape of Devils Tower, defined by the geometry of the host, and (2) the conductive cooling downwards from a surface exposed to the atmosphere, causing decreasing cooling rate with depth (e.g. Hon et al. 1994). Similarly, large columns characterise felsic (rhyolitic, phonolitic) domes and dome-flow structures, with the magma's chemical composition that most commonly control the igneous body's morphology.

Conclusions and perspectives

With the goal of investigating which physical factors control the spacing of columnar joints, we developed a software routine to rapidly process quantitative joint geometries from photographs. The variations in mean side length, mean cross-sectional area and the average polygonal order of columns were measured and analysed for 50 sites. The results show that the range of size variation substantially exceeds one order of magnitude and that all sites with a reasonable amount of data show an average polygonal order below 6. The area–length relationship as a function of the polygonal order shows that the developed network of natural fractures requires expenditure of more energy than needed to produce a regular hexagonal pattern. While such a pattern would result in the most efficient relief of thermal stresses during cooling, the deviation from it seems indicative of non-steady-state cooling resulting in non-equilibrium evolution of the fracture network.

We also focused on two factors likely to play a major role in controlling the characteristic size of columns. One is the geometry of the emplaced magma body and its thickness, which define the boundary conditions to the cooling process. The other is the chemistry of the lava, which controls its physical (mechanical and thermal) properties. Based on the analysis of field examples covering a broad range of chemical compositions, we argue that both controlling factors play an important role in determining L, the characteristic length of column-bounding joints. At comparable chemical compositions, the constraining geometry determines the value of L, depending on the cooling body's boundary conditions as imposed by the geological setting. In the case of unconstrained geometries, such as lava flows, the chemical composition helps control the form of the body and thereby the value of L, with more felsic lavas producing larger columns.

This study suggests two things. First, the database on mean columnar jointing size should be expanded in order to better populate Figs. 10 and 11. One could focus on cooling igneous bodies whose thickness can be measured or estimated more precisely and/or other columnar jointed sites with good

exposure allowing 3D reconstruction of the geometry (e.g. recent, free lava flows). A second aspect of the understanding of columnar jointing formation to be further investigated is the set of conditions for the formation of the entablature and the colonnade in the case of multiple-unit flows (difference in cooling rates, chronology of their formation, ratio of their thickness and characteristic columns size).

Appendix: Comparable cooling regimes for intrusive and extrusive cases: an equivalent thickness ratio

With the objective of comparing the thickness of a simple intrusive (dyke) and extrusive (flow) igneous body having the same cooling regime, we make the following assumptions:

- We place ourselves in a 1D problem along the y-axis (parallel to the temperature gradient).
- Host rock and magma have the same thermal diffusivity κ that does not vary with temperature T.
- The host rock temperature is initially set at 0°C (no preheating of the rock by previous lava).
- There is no latent heat of crystallisation due to solidification.
- The magma is suddenly emplaced at temperature T_0, both in the intrusive and the extrusive case.

For an intrusion of thickness d_i located between $-d_i/2 < y < d_i/2$ and cooling to both sides (country rock in $|y| > d_i/2$), the temperature evolution as a function of depth y and time t is given by Carslaw and Jaeger (1959, p. 54):

$$T(y,t) = \frac{1}{2} T_0 \left[\text{erf}\left(\frac{\frac{d_i}{2} - y}{2\sqrt{\kappa t}} \right) + \text{erf}\left(\frac{\frac{d_i}{2} + y}{2\sqrt{\kappa t}} \right) \right] \quad (4)$$

In the extrusive case, the upper surface of the magma is maintained at 0°C (infinite heat transfer to the air). The lava flow of thickness d_e is located in the region $0 < y < d_e$ and

cools to the host rock located $y > d_e$. With these boundary conditions, the temperature evolution is given by Carslaw and Jaeger (1959, p. 62):

$$T(y,t) = \frac{1}{2} T_0 \left[2\text{erf}\left(\frac{y}{2\sqrt{\kappa t}} \right) - \text{erf}\left(\frac{y - d_e}{2\sqrt{\kappa t}} \right) - \text{erf}\left(\frac{y + d_e}{2\sqrt{\kappa t}} \right) \right] \quad (5)$$

With a change of variable from t to $\tau = \kappa \cdot t/d^2$ and the notation $y^* = y/d$ (where d is, respectively, d_i and d_e for the above cases), the above equations can be written as

$$\Theta_i(y^\star, \tau) = \frac{T\left(\frac{y}{d_i}, \tau \right)}{T_0} = \frac{1}{2} \left[\text{erf}\left(\frac{\frac{1}{2} - y^\star}{2\tau^{\frac{1}{2}}} \right) + \text{erf}\left(\frac{\frac{1}{2} + y^\star}{2\tau^{\frac{1}{2}}} \right) \right] \quad (6)$$

and

$$\Theta_e(y^\star, \tau) = \frac{T\left(\frac{y}{d_e}, \tau \right)}{T_0}$$
$$= \frac{1}{2} \left[2\text{erf}\left(\frac{y^\star}{2\tau^{\frac{1}{2}}} \right) - \text{erf}\left(\frac{y^\star - 1}{2\tau^{\frac{1}{2}}} \right) - \text{erf}\left(\frac{y^\star + 1}{2\tau^{\frac{1}{2}}} \right) \right] \quad (7)$$

We then define the remaining heat as the ratio between mean temperature of the emplaced lava body and the initial temperature T_0. This leads for the intrusive case to

$$E_i(\tau) = \int_{-0.5}^{0.5} \Theta_i(y^\star, \tau) \, dy^\star \quad (8)$$

and for the extrusive case to

$$E_e(\tau) = \int_0^1 \Theta_e(y^\star, \tau) \, dy^\star \quad (9)$$
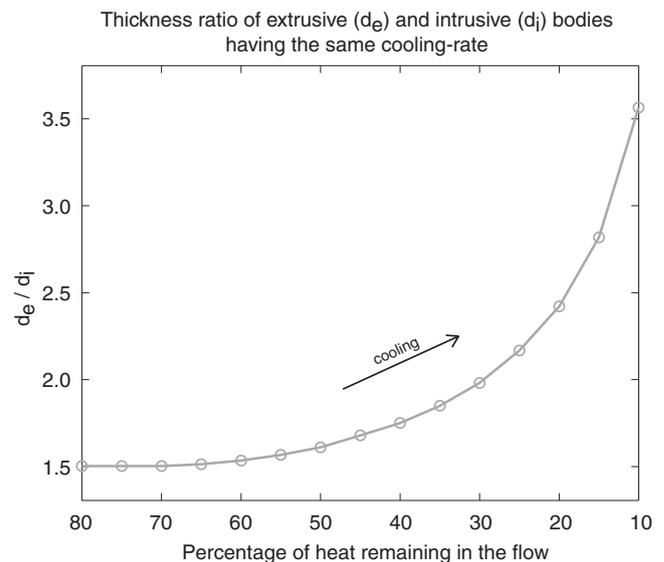

Fig. 12 Thickness ratio of igneous bodies having the same cooling rate, as a function of the remaining heat within the body. See text for details

We numerically integrate Eqs. 8 and 9 and investigate for a given percentage of remaining heat $\in$ the ratio of extrusive thickness d_e to intrusive thickness d_i for which the cooling rate is the same in both magmas bodies at time t:

$$E_i(\tau_i) = \in = E_e(\tau_e), \tag{10}$$

$$E_i\left(t\frac{\kappa}{d_i(\in, t)^2}\right) = E_e\left(t\frac{\kappa}{d_e(\in, t)^2}\right) \tag{11}$$

The result is shown in Fig. 12. We can first see that an extrusion is always required to be thicker than an intrusion cooling at the same rate, whatever the amount of remaining heat in the lava, because a lava flow always cools faster than an intrusive magma body. Second, the smaller the remaining heat in the lava, the higher extrusive/intrusive thickness ratio is required (the more rapid the cooling of a flow compared to a dyke).

As the temperature at emplacement T_0 is near or below the liquidus (in the order of 1,000–1,200°C) and jointing occurs near the glass transition temperature T_G (in the order of 650–950°C with the rock compositions in this paper and using the model by Giordano et al. (2008)), the remaining heat exceeds 50% at that emplacement when jointing takes place. Therefore, when comparing extrusive and intrusive bodies having the same cooling rate, a realistic number with which one should divide the thickness of a dyke (sill) to compare it to that of a free flow is 1.5.

References

Aydin A, DeGraff JM (1988) Evolution of polygonal fracture patterns in lava flows. Science 239:471–476

Bout P (1960) Le Villafranchien du Velay et du bassin hydrographique moyen et supérieur de l'Allier. Imprimerie Jeanne-d'Arc, Le Puy en Velay, 1–344 pp (in French)

Brousse R (1961) Analyses chimiques des roches volcaniques tertiaires et quaternaires de la France. Bull Serv Carte Géol Fr 263(58):1–140 (in French)

Brousse R, Tempier P, Rançon JP, Veyret-Mekdjian Y (1989) Notice explicative, carte géologique de la France (1/50000), feuille Bourg-Lastic. Bureau de Recherches Géologiques et Minières, Orléans, pp 1–78, in French

Brousse R, Rançon JP, Le Garrec MJ, Veyret-Mekdjian Y, Medhizadeh H, Mervoyer B, Musengié M (1990) Notice explicative, carte géologique de la France (1/50000), feuille La Tour-d'Auvergne. Bureau de Recherches Géologiques et Minières, Orléans, pp 1–68 (in French)

Budkewitsch P, Robin PY (1994) Modelling the evolution of columnar joints. J Volcanol Geotherm Res 59:219–239

Bulkeley RB (1693) Part of a letter concerning the Giants Causeway in the County of Atrim in Ireland. Trans Roy Soc London 17:708–710

Büttner R, Dellino P, Raue H, Sonder I, Zimanowski B (2006) Stress-induced brittle fragmentation of magmatic melts: theory and experiments. J Geophys Res 111:B08204. doi:10.1029/2005JB003958

Carslaw HS, Jaeger JC (1959) Conduction of heat in solids. Oxford University Press, Oxford, pp 1–510

Castro JM, Beck P, Tuffen H, Nichols ARL, Dingwell DB, Martin MC (2008) Timescales of spherulite crystallization in obsidian inferred from water concentration profiles. Am Mineral 93:1816–1822

Cheguer L (1990) Interprétation quantitative de la prismation des laves. Master thesis, Université Blaise Pascal, Clermont-Ferrand, 1–45 (in French)

DeGraff JM, Aydin A (1987) Surface morphology of columnar joints and its significance to mechanics and direction of joint growth. Geol Soc Am Bull 99:605–617

DeGraff JM, Long PE, Aydin A (1989) Use of joint-growth directions and rock textures to infer thermal regimes during solidification of basaltic lava flows. J Volcanol Geotherm Res 38:309–324

Demarest N (1774) Mémoire sur l'origine et la nature du basalte à grandes colonnes polygones, déterminées par l'histoire naturelle de cette pierre, observée en Auvergne. Histoire et mémoires de l'Académie Royale des Sciences, Année 1771, Paris, pp 705–775

Demarest N (1777) Mémoire sur le basalte, troisème partie. Histoire et mémoires de l'Académie Royale des Sciences, Année 1773, Paris, pp 599–670

Dingwell DB (1995) Relaxation in silicate melts: some applications. In: Stebbins JF, McMillan PF, Dingwell DB (eds) Structure, dynamics and propertied of silicate melts. Rev Mineral Geochem 32, pp 21–66

Dingwell DB (1996) Volcanic dilemma: flow or blow? Science 273:1054–1055

Dobosi G, Fodor RV, Goldberg SA (1995) Late-Cenozoic alkalic basalt magmatism in Northern Hungary and Slovakia: petrology, source compositions and relationship to tectonics. Acta Vulcanol 7 (2):199–207

Embey-Isztin A, Downes H, James DE, Upton BGJ, Dobosi G, Ingram GA, Harmon RS, Scharbert HG (1993) The petrogenesis of Pliocene alkaline volcanic rocks from the Pannonian Basin, Eastern Central Europe. J Petrol 34(2):317–343

Gilbert CM (1938) Welded tuff in eastern California. Geol Soc Am Bull 49:1829–1862

Gilman JJ (2009) Basalt columns, large scale constitutional super-cooling? J Volcanol Geotherm Res 184:347–350

Giordano D, Russell JK, Dingwell DB (2008) Viscosity of magmatic liquids: a model. Earth Planet Sci Lett 271:123–134

Gméling K, Németh K, Martin U, Eby N, Varga Z (2007) Boron concentrations of volcanic fields in different geotectonic settings. J Volcanol Geotherm Res 159:70–84

Goehring L, Morris SW (2005) Order and disorder in columnar joints. Europhys Lett 69:739–745

Goehring L, Lin Z, Morris SW (2006) An experimental investigation of the scaling of columnar joints. Phys Rev E 74:036115

Goehring L, Mahadevan L, Morris SW (2009) Nonequilibrium scale selection mechanism for columnar jointing. Proc Nat Acad Sci 106(2):387–392

Goër de Hervé A (1972) La planèze de Saint-Flour. Ph.D. thesis, Université Blaise-Pascal, Clermont-Ferrand, 1–244 (in French)

Goto Y, McPhie J (1998) Endogenous growth of a Miocene submarine dacite cryptodome, Rebun Island, Hokkaido, Japan. J Volcanol Geotherm Res 84:273–286

Gray NH (1986) Symmetry in a natural fracture pattern: the origin of columnar joint networks. Comp & Maths with Appls 12B(3/4):531–545

Grossenbacher KA, McDuffie SM (1995) Conductive cooling of lava: columnar joint diameter and stria width as functions of cooling rate and thermal gradient. J Volcanol Geotherm Res 69:95–103

Guillou H, Van Vliet-Lanoë B, Guðmundsson A, Nomade S (2010) New unspiked K–Ar ages of Quaternary sub-glacial and sub-aerial volcanic activity in Iceland. Quat Geochronol 5:10–19. doi:10.1016/j.quageo.2009.08.007

Guy B (2010) Comments on "Basalt columns: large scale constitutional supercooling?" by John Gilman (JVGR, 2009) and presentation of some new data. J Volcanol Geotherm Res 194:69–73

Guy B, Le Coze J (1990) Reflections on columnar jointing of basalts: the instability of the planar solidification front. Comptes rendus de l'Académie des sciences Paris 311(II):943–949

Harangi SZ, Vaselli O, Tonarini S, Szabó CS, Harangi R, Coradossi N (1995) Petrogenesis of Neogene extension-related alkaline volcanic rocks of the Little Hungarian Plain Volcanic Field (Western Hungary). In: Downes H, Vaselli O (eds) Neogene and related magmatism in the Carpatho-Pannonian Region. Acta Vulcanol 7, pp 173–187

Hardarson BS, Fitton JG, Ellam RM, Pringle MS (1997) Rift relocation—a geochemical and geochronological investigation of a palaeo-rift in northwest Iceland. Earth Planet Sci Lett 153:181–196

Hédervári P (1981) Évezredek, vulkánok, emberek (Millennia, volcanoes, men). Univerzum, Budapest, p 310 (in Hungarian)

Hemond C, Arndt N, Lichtenstein U, Hofmann A, Oskarsson N, Steinthorsson S (1993) The heterogeneous Iceland plume: Nd–Sr–O isotopes and trace element constraints. J Geophys Res 98:15833–15850. doi:10.1029/93JB01093

Hon K, Kauahikaua J, Denlinger R, Mackay K (1994) Emplacement and inflation of pahoehoe sheet flows—observations and measurements of active lava flows on Kilauea Volcano, Hawaii. Geol Soc Am Bull 106:351–370

Hull D, Caddock BD (1999) Simulation of prismatic cracking of cooling basalt lava flows by the drying of sol-gels. J Materials Sci 34:5707–5720

Huppert EH, Shepherd JB, Sigurdsson H, Sparks RSJ (1982) On lava dome growth, with application to the 1979 lava extrusion of the Soufrière of St. Vincent. J Volcanol Geotherm Res 14:199–222

Jaeger JC (1961) The cooling of irregularly shaped igneous bodies. Am J Sci 259:721–731

Jakobsson SP (1972) Chemistry and distribution pattern of recent basaltic rocks in Iceland. Lithos 5:365–386. doi:10.16/0024-4937 (72)90090-4

Jaupart C, Allègre CJ (1991) Gas content, eruption rate and instabilities of eruption regime in silicic volcanoes. Earth Planet Sci Lett 102:413–429. doi:10.1016/0012-821X(91)90032-D

Juhász Á (1987) Évmilliók emlékei (Souvenirs of millions of years). Gondolat, Budapest (in Hungarian)

Karner FR, Halvorson DL (1989) Geology of the Devils Tower and Missouri Buttes region. In: Karner FR (ed) Devils Tower—Black Hills alkalic igneous rocks and general geology, field trip guidebook T131. American Geophysical Union, Washington, DC, pp 70–74

Kattenhorn SA, Schaefer CJ (2008) Thermal–mechanical modeling of cooling history and fracture development in inflationary basalt lava flows. J Volcanol Geotherm Res 170:181–197

Kereszturi G, Nemeth K, Csillag G, Balogh K, Kovács J (2011) The role of external environmental factors in changing eruption styles of monogenetic volcanoes in a Mio/Pleistocene continental volcanic field in western Hungary. J Volcanol Geotherm Res 201:227–240. doi:10.1016/j.jvolgeores.2010.08.018

Konrad J-M, Ayad R (1997) Desiccation of a sensitive clay: field experimental observations. Can Geotech J 34:929–942

Kóthay K (2009) The evolution of alkali basaltic magma based on the study of silicate melt inclusions from Hegyestű and Haláp, Balaton Highland. Ph.D. thesis, Dept. of Petrology and Geochemistry, Eötvös Loránd University, Budapest, 1–164 (in Hungarian)

Long PE, Wood BJ (1986) Structures, textures and cooling histories of Columbia River basalt flows. Geol Soc Am Bull 97:1144–1155

Lore J, Gao H, Aydin A (2000) Viscoelastic thermal stress in cooling basalt flows. J Geophys Res 105:23695–23709

Lore J, Aydin A, Goodson K (2001) A deterministic methodology for prediction of fracture distribution in basaltic multiflows. J Geophys Res 106(B4):6447–6459

Mallett R (1875) On the origin and mechanism of production of the prismatic (or columnar) structure of basalt. Proc Roy Soc London 23:180–184

Martin U, Németh K (2004) Mio/Pliocene phreatomagmatic volcanism in the Western Pannonian Basin. Geologica Hungarica Series Geologica 26, Budapest, 1–193, ISBN 963 671 238 7

Martin U, Németh K (2007) Blocky versus fluidal peperite textures developed in volcanic conduits, vents and crater lakes of phreatomagmatic volcanoes in Mio/Pliocene volcanic fields of Western Hungary. J Volcanol Geotherm Res 159:164–178. doi:10.1016/j.jvolgeores.2006.06.010

Martin U, Németh K, Auer A, Breitkreuz Ch, Csillag G (2002) Depositional record of a Pliocene nested multivent maar complex at Fekete hegy, Pannonian Basin, western Hungary. Geologica Carpathica 53: Proceedings of XVII. Congress of Carpathian–Balkan Geological Association, Bratislava, Sept. 1–4th, 2002

Maurizot-Blanc C (1974) Etude des formations volcaniques de la cuvette de Murat et de la vallée de la Chevade. Etude pétrographique et pétrochimique des basaltes miocènes et pliocènes de la planèze de Saint-Flour (Cantal). Ph.D. thesis, University of Grenoble, Grenoble, 1–211 (in French)

Mergoil J, Boivin P (1993) Le Velay. Son volcanisme et les formations associées. Notice de la carte à 1/100 000. Géologie de la France 3:3–96 (in French)

Michon L, Merle O (2001) The evolution of the Massif Central rift: spatio-temporal distribution of the volcanism. Bull Soc Géol France 172:201–211

Mossand P (1983) Le volcanisme anté- et syn-caldeira des Monts-Dore (Massif Central Français). Implications géothermiques. Ph. D. thesis, University Blaise Pascal, Clermont-Ferrand, 1–197 (in French)

Müller G (1998) Starch columns: analog model for basalt columns. J Geophys Res 103:15239–15253

Murase T, McBirney AR (1973) Properties of some common igneous rocks and their melts at high temperatures. Geol Soc Am Bull 84:3563–3592

Mysen BO (1988) Structure and properties of silicate melts. Developments in geochemistry 4. Elsevier, Amsterdam, pp 1–368

Nemeth K, Martin U (1998) Groundwater and gas rich magma controlled phreatomagmatic (maar/diatreme) volcanism in the Balaton Highland Volcanic Field, Pannonian Basin, Hungary. IAVCEI 98 Congress, Cape Town, Abstract book p. 43

Németh K, Martin U (2007) Shallow sill and dyke complex in western Hungary as a possible feeding system of phreatomagmatic volcanoes in "soft-rock" environment. J Volcanol Geotherm Res 159:138–152. doi:10.1016/j.jvolgeores.2006.06.014

O'Reilly JP (1879) Explanatory notes and discussion on the nature of the prismatic forms of a group of columnar basalts, Giant's Causeway. Trans R Irish Acad 26:641–728

Peck DL, Minakami T (1968) The formation of columnar joints in the upper part of Kilauean lava lakes. Hawaii Geol Soc Am Bull 79:1151–1166

Prakfalvi P (2002) A béri hajlott andezitoszlopok. (The bent andesite columns of Bér.) Polár Stúdió, Salgótarján, 1–20 (in Hungarian)

Raspe RE (1776) An account of some German volcanos, and their productions. With a new hypothesis of the prismatic basaltes; established upon facts. Being an essay of physical geography for

philosophers and miners. Published as supplementary to Sir William Hamilton's observations on the Italian volcanos. Lockyer Davis, London, pp 1–140

Ryan MP, Sammis CG (1978) Cyclic fracture mechanisms in cooling basalt. Geol Soc Am Bull 89:1295–1308

Ryan MP, Sammis CG (1981) The glass transition in basalt. J Geophys Res 86:9519–9535

Saemundsson K (1970) Interglacial lava flows in the lowlands of Southern Iceland and the problem of two-tiered columnar jointing. Jökull 20:62–77

Saemundsson K (1986) Subaerial volcanism in the western N. Atlantic. In: Vogt PR, Tucholke BE (eds) The geology of North America, vol. M: the western N. Atlantic region. Geological Society of America, Boulder, pp 69–86

Schmincke HU (2004) Volcanism. Springer, Heidelberg, pp 1–324

Schultz RA (1995) Limits on strength and deformation properties of jointed basaltic rock masses. Rock Mech Rock Engng 28:1–15

Sigmarsson O (2007) Origin of Icelandic basalts: a review of their petrology and geochemistry. J Geodynamics 43:87–100

Sigvaldason GE (1974) Basalts from the centre of the assumed Icelandic mantle plume. J Petrol 15:497–524

Sosman RB (1916) Types of prismatic structures in igneous rocks. J Geol 24:215–234

Spörli KB, Rowland JV (2006) 'Column on column' structures as indicators of lava/ice interaction, Ruapehu andesite volcano, New Zealand. J Volcanol Geotherm Res 157:294–310. doi:10.1016/j.jvolgeores.2006.04.004

Spry AH (1962) The origin of columnar jointing, particularly in basalt flows. J Geol Soc Aust 8:191–216

Spry AH, Solomon M (1964) Columnar buchites at Apsley, Tasmania. Quart J Geol Soc 120:519–544. doi:10.1144/gsjgs.120.1.0519

Tardy J, Barczi A, Brezsnyánszky K, Császár G, Eszterhás I, Harangi Sz, Hámor G, Izsó I, Kordos L, Prakfalvi P, Szarvas I (2009) Novohrad-

Nográd Geopark, Geology I. Enclosure to the application dossier for nomination as a European Geopark. http://ipolytarnoc.kvvm.hu/uploads/File/pdf/NNG_Enclosure_5.pdf. Cited on 21 Sep 2009

Thorarinsson S (1981) Miscellanea from excursions through south Iceland. Jökull 31:65–81 (in Icelandic)

Tomkeieff SI (1940) The basalt lavas of the Giant's Causeway district of Northern Ireland. Bull Volcanol 6:89–146

Toramaru A, Matsumoto T (2004) Columnar joint morphology and cooling rate: a starch–water mixture experiment. J Geophys Res 109:B02205. doi:10.1029/2003JB002686

Turcotte DL, Schubert G (2002) Geodynamics, 2nd edn. Cambridge Univ. Press, Cambridge, pp 1–456

Varet J (1967) Les trachytes et les phonolites du Cantal Septentrional. Ph.D. thesis, Université de Paris, Faculté des Sciences d'Orsay, Orsay, 1–195 (in French)

Varet J (1971) Structure et mise an place des massifs phonolitiques du Cantal (Auvergne, France). Geol Rundschau 60(3):948–970

Varet J (1975) A propos des phonolites de Bort (Corrèze). Compte Rendu Somm Soc Géol France 17–4:99–101 (in French)

Vink GE (1984) A hotspot model for Iceland and the Voring Plateau. J Geophys Res B 89:9949–9959

Walker GPL (1967) Thickness and viscosity of Etnean lavas. Nature 213:484–485

Walker GPL (1973) Lengths of lava flows. Phil Trans R Soc Lond A 274:107–118

Wijbrans J, Németh K, Martin U, Balogh K (2007) 40Ar/39Ar geochronology of Neogene phreatomagmatic volcanism in the western Pannonian Basin, Hungary. J Volcanol Geotherm Res 164:193–204. doi:10.1016/j.jvolgeores.2007.05.009

Woodworth JB (1896) On the fracture system of joints, with remarks on certain great fractures. Proc Boston Soc Nat Hist 27:163–184

Zarzycki J (1982) Les verres et l'état vitreux. Masson, Paris, pp 1–391 (in French)